Fluids and Barriers of the CNS

REVIEW

Open Access

A review of cerebrospinal fluid circulation with respect to Chiari-like malformation and syringomyelia in brachycephalic dogs

Ryan Jones[1*], Srdjan Cirovic[2] and Clare Rusbridge[1,3]

Abstract

Cerebrospinal fluid (CSF) plays a crucial role in maintaining brain homeostasis by facilitating the clearance of metabolic waste and regulating intracranial pressure. Dysregulation of CSF flow can lead to conditions like syringomyelia, and hydrocephalus. This review details the anatomy of CSF flow, examining its contribution to waste clearance within the brain and spinal cord. The review integrates data from human, canine, and other mammalian studies, with a particular focus on brachycephalic dogs. Certain dog breeds exhibit a high prevalence of CSF-related conditions due to artificial selection for neotenous traits, making them valuable models for studying analogous human conditions, such as Chiari-like malformation and syringomyelia associated with craniosynostosis. This review discusses the anatomical features specific to some brachycephalic breeds and the impact of skull and cranial cervical conformation on CSF flow patterns, providing insights into the pathophysiology and potential modelling approaches for these conditions.

Keywords Brachycephaly, CSF flow system, Glymphatic, Canine CSF anatomy, Craniosynostosis, Subarachnoid space, Choroid plexus, Incidence, Mesencephalic aqueduct

Introduction

Cellular metabolic activity generates waste, which requires clearance to maintain tissue homeostasis. Within the brain, waste clearance is facilitated by cerebrospinal fluid (CSF), an ordinarily clear fluid composed of inorganic ions, proteins, glucose, and cells [1]. This fluid flows in a pulsatile manner within fluid-cavities of the brain and spinal cord, performing a variety of functions; elimination of waste metabolites, dampening of hydraulic shock, and buffering of intracranial pressure changes [2]. As such, conditions associated with CSF flow dysregulation (Chiari(-like) malformation, syringomyelia, hydrocephalus, etc.) have the potential to be severely detrimental to health. This review presents the fluid system in terms of macroscale bulk CSF flow components within the brain and spinal canal, and in terms of microscale components which facilitate the metabolite exchange and waste clearance. Human, canine, and other mammalian data are reviewed focussing on common traits.

The CSF flow system is next discussed in the context of two CSF related conditions (Chiari(-like) malformation and syringomyelia) in brachycephalic dogs. Owing to artificial selection for neotenous characteristics in breeding, such dogs have extremely high prevalence of CSF related conditions when compared to humans. Therefore, brachycephalic dogs offer a unique opportunity to study conditions analogous to human craniosynostosis-related

*Correspondence:
Ryan Jones
rj00642@surrey.ac.uk
[1] School of Veterinary Medicine, University of Surrey, Guildford GU2 7XH, UK
[2] Department of Mechanical Engineering Sciences, University of Surrey, Guildford GU2 7XH, UK
[3] Wear Referrals Veterinary Specialist & Emergency Hospital, Bradbury, Stockton-On-Tees, UK

disorders, serving as a "spontaneous model" for Chiari-like malformation and syringomyelia. Specific anatomical features, their effect on CSF flow patterns, related pathological conditions, prevalence, and clinical outcomes are discussed.

Macroscale flow

CSF flow is highly complex, exhibiting temporal and spatial variations in velocity and direction [3]. Classically, as per the Weed-Dandy-Cushing CSF flow hypothesis, it was generally accepted that CSF flows unidirectionally (caudally directed) through the ventricular system. However, this convention is under significant scrutiny with contemporary evidence favouring a bidirectional flow system [4–7].

The ventricular system, shown in Fig. 1 is comprised of fluid-filled cavities located within the brain and spinal parenchyma, extending to an auxiliary cavity at the caudal end of the spinal cord. The lateral ventricles are connected to the third ventricle by the intraventricular foramen (foramen of Monro in humans) which is, in turn, connected to the fourth ventricle via the mesencephalic (cerebral) aqueduct. The ventricular system concludes at the terminal ventricle, which is connected to the fourth ventricle via the central canal of the spinal cord and is located at the conus medullaris. There is evidence that the terminal ventricle and spinal subarachnoid space (SAS) are communicating in the dog [8], however, this is not the case for all mammalian species [9]. The fluid cavities of the ventricular system are open and communicating, permitting the movement of fluid within the brain and spinal cord [10]. It should be noted that, while the central canal is patent in dogs [8, 11], this is not generally the case in adult humans [12, 13]. In dogs, the mesencephalic aqueduct is distended towards the rostral aspect of the cerebellum. This presents as an additional pyramidal fluid-filled cavity between the third and fourth ventricles bounded caudally by the rostral lobe of the cerebellum, dorsally by the tectum, and ventrally by the tegmentum of the midbrain. This cavity is separate yet connected to the mesencephalic aqueduct, seemingly innominate within veterinary literature, and may affect fluid flow within the aqueduct.

CSF is also present within the meningeal structures, specifically within the SAS which surrounds the brain and spinal cord. This space is bound by the pia mater

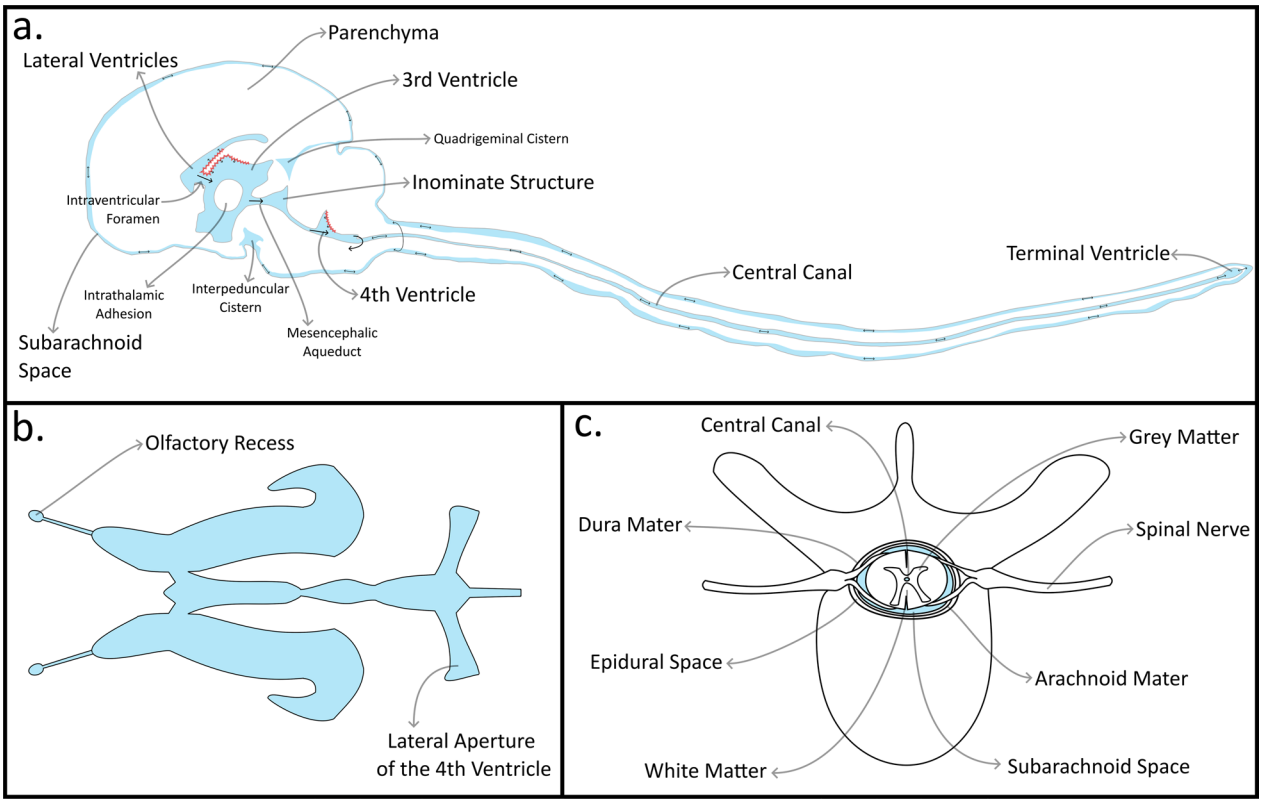

Fig. 1 The macroscale cerebrospinal fluid (CSF) flow system; key anatomical locations for studying canine CSF flow; **a** The brain and spinal cord in the mid-sagittal plane, red indicates the choroid plexus, black arrows indicate flow directionality. **b** The ventricular system in the coronal plane. **c** The spinal canal in the transverse plane

(inner), and dura mater (outer), which are connected by arachnoid trabeculae. As such, the SAS is characterised as porous, with CSF flowing around the arachnoid trabeculae network [14]. *Eide & Ringstad, 2024* found that the SAS is compartmentalised by a semipermeable membrane in humans, allowing for directed transport of solutes along cerebral arteries [15]. A similar observation has been made in mice [16, 17]; however, this finding has been contested [18–21]. The ventricular system and SAS are contiguous [22], connected at the lateral apertures of the fourth ventricle (also termed the foramen of Luschka), some species (including primates and some rodents) possess an additional pathway called the foramen of Magendie, which extends posteriorly from the fourth ventricle. This opening is not present in dogs [23].

Recent evidence favours pulsatile multidirectional CSF flow. Ependymal cells lining the ventricles contain cilia which project into the CSF, these cilia may drive complex intraventricular circulatory flow patterns within the ventricles [24, 25]. There is evidence to suggest that cilia motion generates bidirectional flow in embryos, ensuring the proper formation of the central canal [26]. In a computational study, *Siyahhan,* et al*., 2014* investigated flow within the lateral ventricles, finding that near-wall flow dynamics are dominated by ependymal cilia action and that macroscale pulsatile flow was driven by ventricular expansion and contraction, in addition to choroid plexus influx [27], see section: Choroid Plexus Influx. Oscillations permit the bidirectional exchange of fluid across different anatomical regions and can be perturbed by a multitude of systems over different characteristic timescales (cardiac $\sim 10^{0}Hz$, respiratory $\sim 10^{-1}Hz$, functional hyperemia (cerebral blood flow coupled to neural metabolic activity) $\sim 10^{-2}Hz$ [22]), the predominate driving forces of pulsatile CSF movement are the cardiac and pulmonary systems [28–30].

CSF flow is coupled to the cardiac cycle [31–33]. *Feinberg,* et al*., 1987* used quantitative Magnetic Resonance Imaging (MRI) to measure CSF flow directionality, discovering vascular-driven movement of the brain parenchyma [34]. During systole, the influx of blood into the brain's vasculature compresses the ventricular system and the SAS within the cranium. This results in caudally directed CSF flow through the foramen magnum and along the spinal SAS. During diastole, as cerebral blood volume decreases, CSF flow is directed rostrally [35], this system is shown in Fig. 2b. *Alperin* et al*. 2000* further demonstrated synchronized flow patterns between arterial inflow, venous outflow, and transcranial CSF flux throughout the cardiac cycle. They observed an

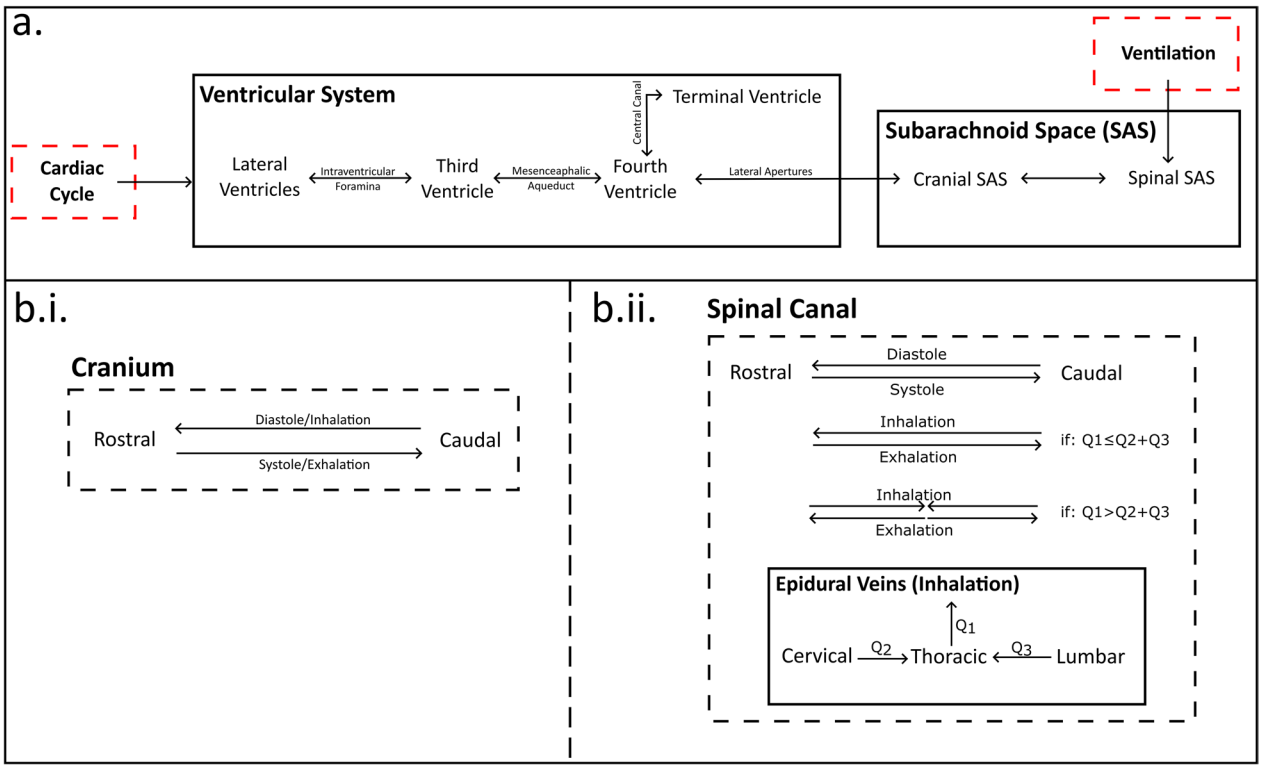

Fig. 2 A system diagram of the **a** total macroscale CSF flow system. **b** Perturbations driven by the cardiac and pulmonary systems within the i. cranial and ii. spinal subarachnoid space (SAS). Q indicates the volumetric flow rate of blood within the epidural venous system during inhalation

imbalance between net arterial influx and net venous and CSF efflux during the cardiac cycle. The sum of the volumes of brain tissue, CSF, and blood was constant when averaged over a cardiac cycle, but not at each instant of time. These observations were used to quantify cranial volume fluctuations over the cardiac cycle and determine cranial compliance; a measure of volumetric change per unit of applied pressure [36].

Ventilation also plays a role in instigating CSF flow due to changes in intrathoracic and abdominal pressure. It generally accepted that CSF flows rostrally during inhalation, and caudally in exhalation [28, 37, 38], this has been explained as a consequence of the Monro-Kellie doctrine; rostral CSF flow during inhalation compensates for the simultaneous venous drainage from the head and neck, driven by reduced intrathoracic pressure [39]. However, this may be an oversimplification, as spinal epidural veins play a significant role in the relationship between CSF dynamics and intrathoracic pressure. Epidural veins are present throughout the entire length of the spinal canal, these veins are a factor in determining the directionality of CSF flow within the spinal canal. As these veins are valveless, flow can initiate within the vessels in any direction allowing them to transmit pressure differences between systems; illustrated in Fig. 2b, in which Q represents fluid flux. Lloyd, et al., 2020 found that during inhalation, negative intrathoracic pressure pulls venous blood towards the thorax, draining the thoracic epidural veins, see Q1; Fig. 2bii. The drained blood volume is replaced by flow from the cervical and lumbar epidural veins (Q2 and Q3 respectively; Fig. 2bii), if the efflux from the thorax is greater than the cumulative influx from the lumbar and cervical veins, bidirectional CSF flow is observed flowing rostrally from the lumbar spine and caudally from the cervical spine ($Q1 > Q2 + Q3$; Fig. 2bii). This is due a reduction in subarachnoid pressure increasing the capacity of the spinal canal; greater efflux from the thoracic epidural veins reduces the epidural space, decreasing the pressure of the thoracic spinal canal inhibiting rostral displacement of cervical CSF and increasing rostral displacement in the lumbar spinal canal. During exhalation, abdominal and intrathoracic pressures return to their resting state, so CSF flows in the opposing direction to the inspiratory case. Conversely, if the efflux from the thoracic epidural veins is less than or equal to the cumulative efflux from the cervical and lumbar regions ($Q1 \leq Q2 + Q3$, Fig. 2bii), the conventionally accepted flow is observed [40]. The influence of the epidural venous plexus on CSF dynamics has also been observed in alligators, for which the effects of respiration are amplified due to their lack of epidural fat. Taylor et al. observed a direct link between epidural and CSF pressures, particularly within the spinal canal, whereas in the cranium cardiac pulsations were dominant. However, it is expected that differences in the spinal venous anatomy create a more complex relationship between the venous and CSF systems in alligators than humans, and indeed, dogs [41]. There is also evidence that that ventricular CSF flow is affected by ventilation. Spijkerman et al. used phase contrast MRI to observe net CSF flow in the mesencephalic aqueduct, finding caudally directed net flow in exhalation, and rostrally in inhalation [42].

The cardiac and pulmonary systems drive CSF on different timescales. Higher frequency cardiac driven CSF velocity is greater than ventilation induced flow, whereas lower frequency ventilation driven fluid exhibits greater displacement of the CSF [43]. Additionally, in the lumbar region, cardiac driven flow is at near-zero velocity, significantly less than ventilation driven flow. Therefore, ventilation dominates flow in the lumbar region [37].

Figure 2 summarises this macroscale CSF flow system highlighting flow directionality, and the impact of cardiac and pulmonary systems on CSF circulation within the cranial and spinal SAS.

Valsalva manoeuvre and cough

During normal breathing, inhalation is associated with negative thoracic pressure, during exhalation the thoracic pressure is driven towards equilibrium; however, the dynamics of this system are sensitive to abrupt manoeuvres like coughing, sneezing, or Valsalva manoeuvre. Coughs and sneezes are known to generate CSF movement [44, 45] Abrupt increases in intrathoracic and intraabdominal pressure generates blood flow into the spinal canal, compressing the spinal dura and driving CSF rostrally [40]. Similarly, a Valsalva manoeuvre describes a case of increased thoracic pressure when exhaling against the glottis driving blood from the thorax to the epidural veins. This compresses the spinal dura, and results in the movement of CSF within the spinal SAS [46]. There are four phases associated with the Valsalva manoeuvre: 1. increased intrathoracic pressure, 2. reduced venous return, followed by baroreflex activation, 3. Pulmonary vasculature refills with blood, 4. Increased venous return [47]. During phases 1 and 2, spinal CSF pressure increases due to the distension of the epidural veins, higher spinal pressure relative to intracranial pressure decreases the flow of CSF across the foramen magnum. During phases 3 and 4, breathing returns to normal. Spinal pressure decreases due to the collapse of the epidural veins, higher intracranial pressure relative to spinal pressure promotes CSF flow across the foramen magnum. Generally, CSF flow between the head and spine decreases during, and increases immediately, after the Valsalva manoeuvre [48].

Microscale flow

Choroid plexus influx

The choroid plexus is a highly vascular epithelium which lines some of the internal surface of the cerebral ventricles, composed of a monolayer of epithelial cells lined with microvilli to increase the functional surface area. They function as a site of influx of CSF into the ventricular system, consisting of two-phases; passive ultrafiltration of blood plasma across fenestrated capillaries, and active transport into the ventricles [4], illustrated in Fig. 3. The precise molecular mechanisms through which choroidal plexus secretion are a matter of debate [49, 50], however it is generally accepted that the influx is dependent on the exchange of ions and H_2O between the ventricular CSF and the interstitial space of the choroid plexus. The classical (Weed-Dandy-Cushing) CSF flow hypothesis postulates that all/most of the CSF influx to the ventricular system originates in the choroid plexus [51], however, this traditional view has been increasingly scrutinized, with debates surrounding the relative contribution of the choroid plexus to overall CSF influx [52–58]. Despite these debates, it remains widely accepted that the choroid plexus serves as a key site of CSF production. In the dog, the choroid plexus of the fourth ventricle comprises around 55% of the total choroid plexus surface area, with the lateral ventricles contributing 38% and third ventricle only 7% [59]. Consequently, the fourth ventricle is likely a critical site of CSF influx [49].

The glymphatic system

The CSF of the brain and spine is in continuous exchange with the interstitial fluid of the parenchyma, facilitating the clearance of interstitial solutes. The system through which rapid exchange of CSF and interstitial fluid occurs has been termed the glymphatic system, due to its functional parallels with the lymphatics system.

As depicted in Fig. 4c, at the cortical surface cerebral arteries branch into pial arteries which run throughout the SAS, these arteries penetrate the brain parenchyma branching further into arterioles. Penetrating arterioles are surrounded by a para-vascular space (also termed the Virchow-Robin space, or peri-vascular space in some literature) containing CSF, forming a continuous network with the CSF of the SAS [60].

Since its initial description in the mid 1800's [61–63], evidence for fluid exchange across the para-vascular space has long been debated. In an early investigation, Weed observed the retrograde passage of fluid from the venous system to the parenchyma, suggesting the existence of a space associated with the cerebral blood vessels

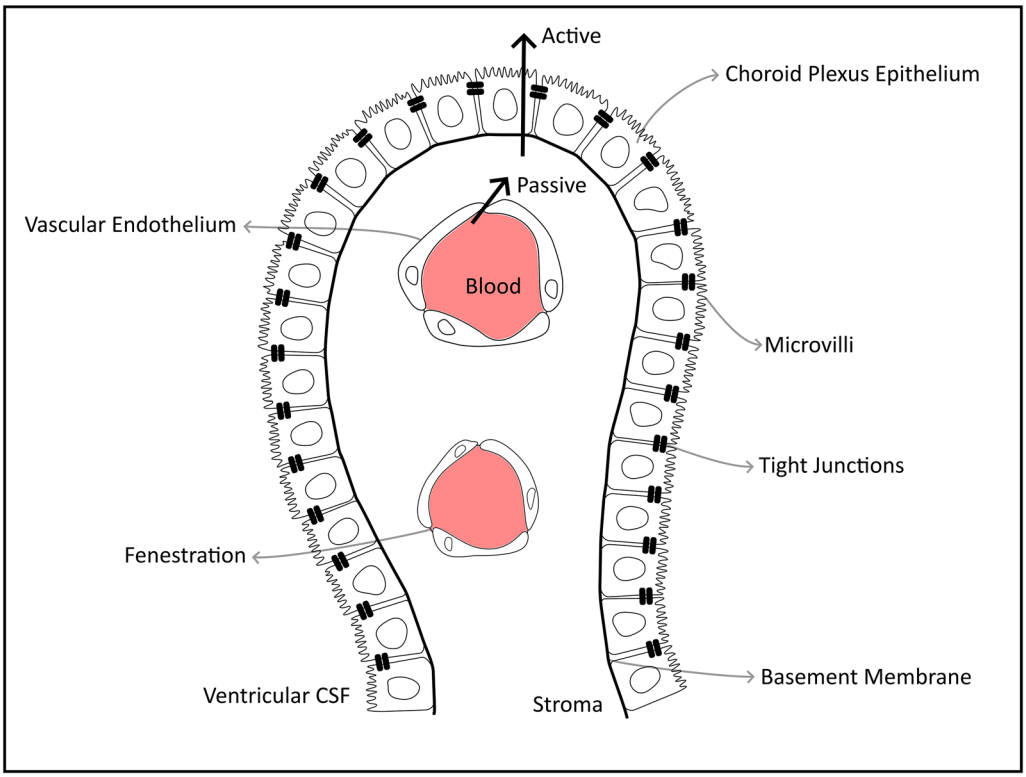

Fig. 3 Anatomy of the choroid plexus, indicating the route of cerebrospinal fluid production; passive ultrafiltration of plasma across fenestrated capillaries, and active transport across the choroid plexus epithelium

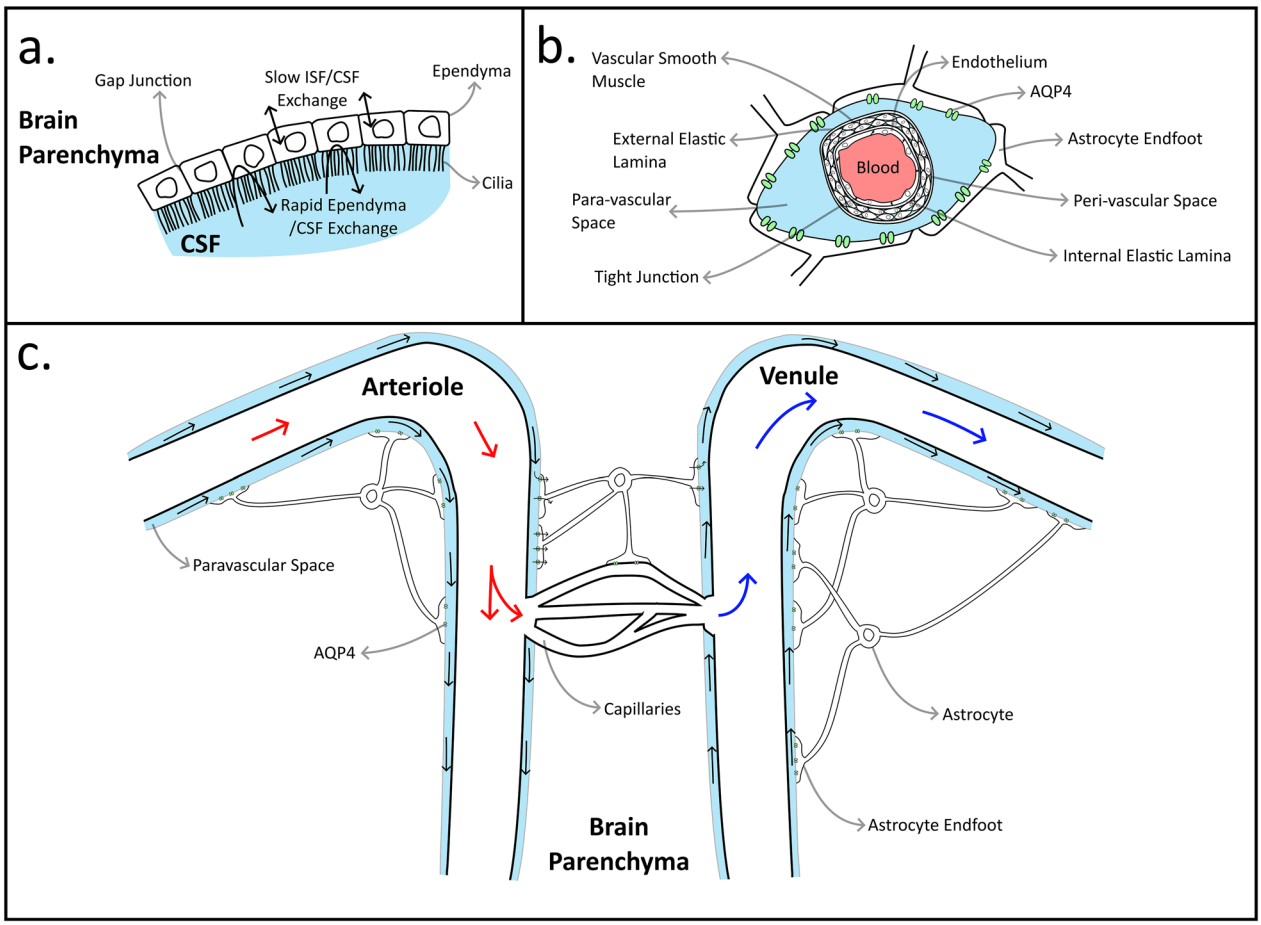

Fig. 4 The glymphatic system. **a** Trans-ependymal fluid exchange within the internal surface of the ventricles. **b** Transverse anatomy of the para-vascular space surrounding penetrating vessels. **c** Glymphatic fluid exchange across the outer brain parenchyma and surface vessels

[64]. For much of the twentieth century, it was generally accepted that fluid efflux from the parenchyma was via "preferred routes", including the para-vascular space [65, 66]. In this hypothesis, solutes were moved through the para-vascular space via diffusion, but along these preferred routes by dispersion (a combination of advection and diffusion) [67]. This hypothesis began to shift as studies indicating that the para-vascular space also functions as an influx route emerged [68, 69]. Iliff et al. investigated the entrance of CSF into the brain parenchyma using various *in-vivo* imaging techniques. Their study concluded that bulk flow facilitates the transport of amyloid-beta through the brain interstitial space, and that this transportation was inhibited by the reduction of aquaporin-4 water channels achieved through deletion of the Aqp4 gene [70]. This has implications for the development of neurodegenerative diseases which have been associated with the accumulation of certain waste proteins (amyloid-beta, tau, alpha-synuclein) [71]. For a more comprehensive review of early investigations into the para-vascular space, readers are directed to Wardlaw et al. and Hladky and Barrand [67, 72].

The para-vascular space is bound internally by the blood vessel basal membrane, and externally by astrocyte end-feet, which contain aquaporin-4 water channels. These channels have been proposed to facilitate the entry of CSF into brain parenchyma, enabling metabolite exchange through more rapid osmosis [22, 73], however the evidence for this is contested [74]. Astrocyte end-foot size is proportional to blood vessel diameter, this variation is predicted to maintain near constant flux of fluid from the para-vascular space to the extracellular space of the parenchyma [75]. According to the glymphatic hypothesis, CSF in the para-arterial space may enter the parenchyma across astrocyte end-feet to exchange with interstitial fluid. The fluid then moves through the interstitium towards the para-venous space where it may efflux across astrocyte end-feet. This proposed bulk flow across the parenchyma from the para-arterial to para-venous spaces results in

the clearance of solutes from the parenchyma to the venous system, however, evidence for bulk flow across the parenchyma is heavily debated [57, 67].

The shape of the para-vascular space is critical for maintaining function (Fig. 4b). Rivas et al. found that the para-vascular space of surface arteries are open [76]. For an open channel, cross-sectional geometry affects the hydraulic resistance [77]. In leptomeningeal arteries, the outer boundary of the para-vascular space is flattened in the direction perpendicular to the skull, reducing the mean wall shear stress and hydraulic resistance by allowing a greater volume of fluid to be further from the vascular wall. With sufficient flattening, the outer wall can contact the vessel wall, dividing the para-vascular space into two distinct domains [22, 77, 78]. As penetrating arterioles branch into the cortex, para-vascular spaces become continuous with the basal lamina of the associated vessel. This is a porous matrix that provides continuity between the fluid spaces of the arterioles and venules [79]. For a channel filled with porous medium, cross-sectional shape does not affect hydraulic resistance provided cross-sectional area is held constant [22].

Net CSF flow within the para-vascular space is antegrade to the direction of blood flow within the associated blood vessel [60], and is characteristically pulsatile. Some studies attribute this pulsatile CSF flow to peristaltic pumping of the arterial vessel wall. In the proximal sections of major cerebral arteries, this flow is driven by the wave-like motion of the arterial walls, while in distal regions, it is propelled by an oscillating pressure gradient created by upstream pumping [80–83]. Conversely, Kedarasetti et al., found that, while peristalsis may drive oscillatory flow within the para-vascular space, net directional flow is driven by pressure gradients present in the system [84]. Other driving mechanisms such as functional hyperaemia, vasomotion (spontaneous arterial wall motion due to the contraction of vascular smooth muscle cells), and ventilation likely contribute to flow dynamics on differing timescales [85].

Within the ventricular system, the CSF may exchange with the interstitial fluid of the parenchyma across ependymal cells which line the internal surface of the ventricles, depicted in Fig. 4a. There is rapid exchange of H_2O between the intercellular fluid in the ependyma, and the CSF of the ventricles. Exchange between the intercellular fluid and interstitial fluid is comparatively slower [86]. This system of trans-ependymal flow provides a constant influx and efflux of fluid across the internal surfaces of the ventricles and has been observed by several studies [87, 88]. Strecker et al. used quantitative audio-radiography to examine the migration of labelled albumin into the periventricular extracellular space in normal and hydrocephalic dogs. Additionally, they found that diffusion was likely the mechanism of transport in the normal dog [89].

Intramural peri-arterial drainage (IPAD)

In addition to glymphatic circulation, another potentially complimentary theory of interstitial fluid drainage has been proposed [7, 90–92]. The IPAD model suggests that interstitial fluid and waste solutes are cleared via the peri-arterial space, this space lies between the layers of vascular smooth muscle cells and basement membranes of penetrating arterioles and is distinct from the para-vascular space (Figs. 4b, 5). Interstitial solutes enter the peri-arterial space and move through the vessel wall retrograde to arterial blood flow [93]. Carare et al. observed the diffusive movement of soluble fluorescent tracers along the basement membranes of capillaries and arteries, indicating the peri-vascular clearance of solutes from the brain.

This flow is driven by vasomotion of the vascular smooth muscle cells, pushing fluid in the direction of the contraction wave, which propagates from the intracerebral arterioles towards large surface arteries [94]. Figure 6 shows a system diagram that integrates both the IPAD and glymphatic systems. For an extensive review of the glymphatic and IPAD systems, readers are directed to Hladky and Barrand [67].

Efflux routes

Lymphatic efflux

It is known that CSF can efflux from the brain and spine via the lymphatic system, where it returns to the venous system [95–98]. However, the precise routes of egress are under debate.

There is evidence that CSF can efflux from the brain through perineurial sheaths surrounding cranial nerves. Direct continuity exists between the cranial SAS, and

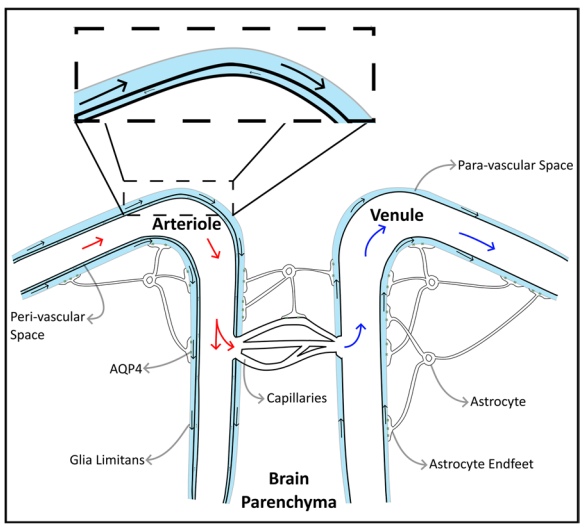

Fig. 5 Intramural peri-arterial drainage (IPAD) fluid exchange across the outer brain parenchyma and surface vessels

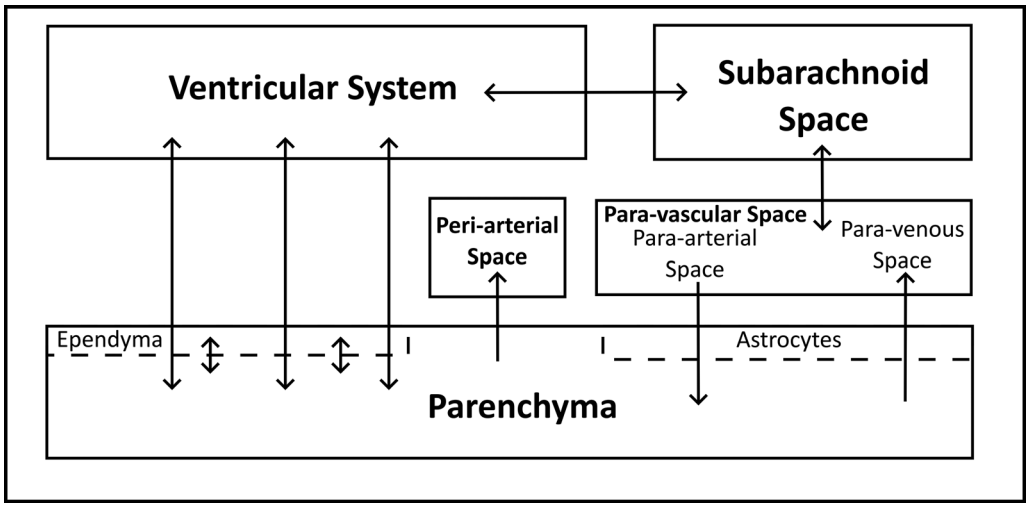

Fig. 6 A systems diagram integrating the glymphatic and Intramural peri-arterial drainage (IPAD) pathways

perineurial sheath of the olfactory nerve (I). This facilitates the flow of CSF across the cribriform plate to the nasal mucosa into nasal lymphatics. Murine studies have found that these lymphatics drain further to cervical lymph nodes, and appear to be a major efflux pathway of CSF [99–101]. Walter et al. investigated the distribution of India ink when injected into the SAS of the rat brain. They found that CSF drains to the nasal lymphatics along olfactory nerves, eventually draining into cervical lymph nodes [102]. Furthermore, Zakharov et al. identified direct continuity between the SAS and perineurial space of the olfactory nerve [103].

The optic nerve (II) is enclosed by a SAS, through which CSF flow has been observed [69, 104, 105]. de la Motte investigated optic nerve associated lymphatics in rabbits via light and electron microscopy. They found that tracer is carried by CSF flow into the SAS of the optic nerve, eventually draining into the deep cervical lymph nodes [106]. However, Lüdemann et al. found that CSF in the optic nerve sheath drains into orbital tissue via an interstitial route, ultimately flowing to conjunctival lymphatic vessels [104].

Ma et al. demonstrated that the trigeminal nerve (V) exhibits a perineurial pattern in mice, and as such represents a potential efflux route for CSF from the cranial SAS to the orbit [96]. This study also demonstrated tracer efflux associated with the facial nerve (VII), draining towards the mandibular and deep cervical lymph nodes. Additionally, there is some evidence that the vestibular nerve (VIII) plays a role in CSF efflux in rabbits, however, this route of efflux requires more investigation [107]. Finally, studies have shown that CSF efflux may occur through the jugular foramina. This route is associated with three cranial nerves, the glossopharyngeal (IX), vagus (X), and accessory (XI). These vessels then drain into the deep cervical lymph nodes [96].

The meningeal lymphatics system represents a further extensive route of CSF clearance in the brain. This system consists of a network of thin, elastic meningeal (dural) lymphatic vessels filled with viscous fluid, which drains due to elastic deformation of the vessel walls [108]. In the rostral (anterior) cranium, meningeal lymphatic vessels are located in the dura covering the olfactory recesses, and are associated with the rostral and middle meningeal arteries. In the caudal and skull base, meningeal lymphatic vessels are found along the sigmoid and transverse sinuses, and in the basal dura overlaying the cerebellum [109]. The meningeal lymphatics system drains to the deep cervical lymph nodes [110].

Lymphatic vessel morphology is dependent on the vessel location, as such dorsal and basal meningeal lymphatic vessels are structurally distinct. Dorsal meningeal lymphatic vessels are located within dural folds along the superior sagittal and transverse sinus, they are structurally comprised of a continuously sealed zipper-like pattern of endothelial cells. By contrast, basal meningeal lymphatic vessels are located along the petrosquamosal and sigmoid sinuses, and are composed of a discontinuously sealed button-like pattern of endothelium. Comparatively, basal meningeal lymphatics possess a larger vessel diameter than their dorsal counterparts. Furthermore, unlike dorsal meningeal lymphatic vessels, basal lymphatics exhibit extensive blunt-ended capillary branches associated with the SAS of the cranium. These morphological differences suggest that basal meningeal lymphatics are more likely to be involved in macromolecular drainage and CSF drainage [96].

Lymphatic vessels are also involved in the clearance of CSF from the SAS of the spine. A network of meningeal lymphatic vessels predominately associated with spinal nerve routes has been described at the cervical and 1st thoracic vertebrae. This network drains to the deep cervical and prevertebral lymph nodes [111]. In the rest of the spine, murine studies have found evidence of continuity between the SAS of the spinal cord, and lymphatic system [112].

Arachnoid villi

Arachnoid villi (or granulations depending on their size) are known to drain a small portion of CSF [113], these are arachnoid membrane projections into the dural sinuses and lateral lacunae comprised of collagen connective tissue and arachnoid cell clusters. The arachnoid granulations act as unidirectional pressure-dependent valves, when CSF pressure exceeds venous pressure, flow is permitted to the venous sinus. In the case that intravenous pressure is greater than CSF pressure, the arachnoid villi collapse closing the valve and inhibiting flow into the sinuses [114, 115]. As such, the arachnoid granulations function as accessory drainage sites in cases of increased intracranial pressure in mice [116] and dogs [117].

It was originally thought that that the arachnoid granulations represent a major site of CSF efflux, however, recent contradictory evidence indicated that these sites contribute to a lesser degree than initially proposed. An MRI study by Radoš et al. revealed significant age-related variability in the number, size, and distribution of arachnoid granulations. Notably, some individuals displayed no arachnoid granulations in their dural sinuses, suggesting that their absence does not impair intracranial homeostasis. This finding indicates that arachnoid granulations are not essential for CSF efflux [118], it is worth noting that their methodology would not detect the smaller arachnoid villi. In the dog, Schurr, et al., 1953 studied the effect obliteration of the SAS by covering the surface with gauze. They observed that blocking efflux sites associated with arachnoid villi did not induce signs of hydrocephalus unless the optic and olfactory routes were also obstructed [119].

Choroid plexus efflux

The choroid plexus is considered to be an accessory site of CSF efflux [120, 121]. A murine study by Akai et al. found that colloidally dispersed gold particles effluxed from the CSF of the lateral ventricles. It was postulated that this clearance was regulated by molecular size [122].

The various efflux routes presented are illustrated schematically in Fig. 7.

Total flow system

A schematic of the total CSF system is presented in Fig. 8, which encapsulates the key anatomical pathways involved in CSF influx, circulation, and efflux. Arrows indicate the fluid flow directionality; this clearly shows the contemporary progression towards a multidirectional fluid flow system with multiple different subsystems.

Influencing factors

Sleep

The parenchyma of the brain is porous, and can therefore be described by its volume fraction, a ratio of the extracellular space and total volumes. However, the volume fraction of the extracellular space of the brain is dynamic and is sensitive to several different states (E.g. sleep, spreading depolarisation, and epilepsy [22]). Using in-vivo imaging, Xie et al. explored the effect of sleep state on the clearance of amyloid-beta from the murine brain. They found that the sleep state is associated with a 60% increase in the interstitial space, driving a significant increase in waste protein exchange [123]. Furthermore, Bojarskaite et al. hypothesised that different parts

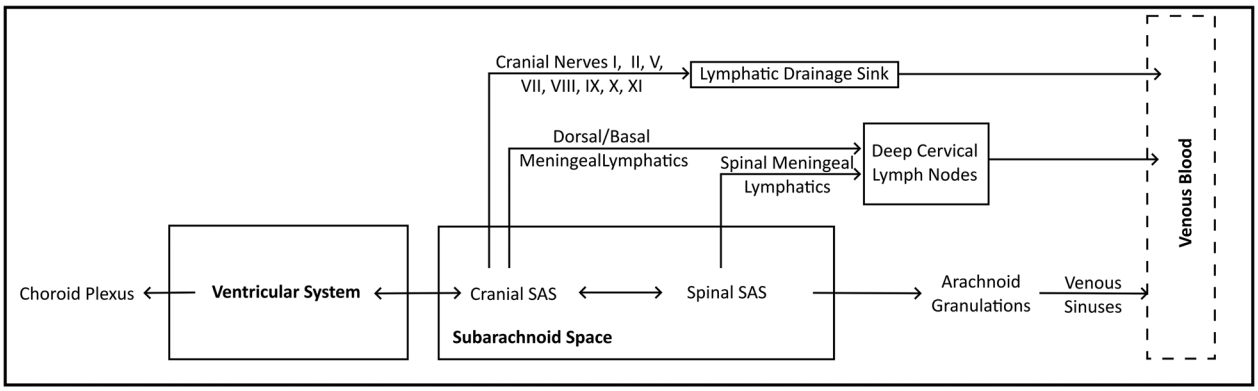

Fig. 7 A system diagram of the cerebrospinal fluid efflux routes

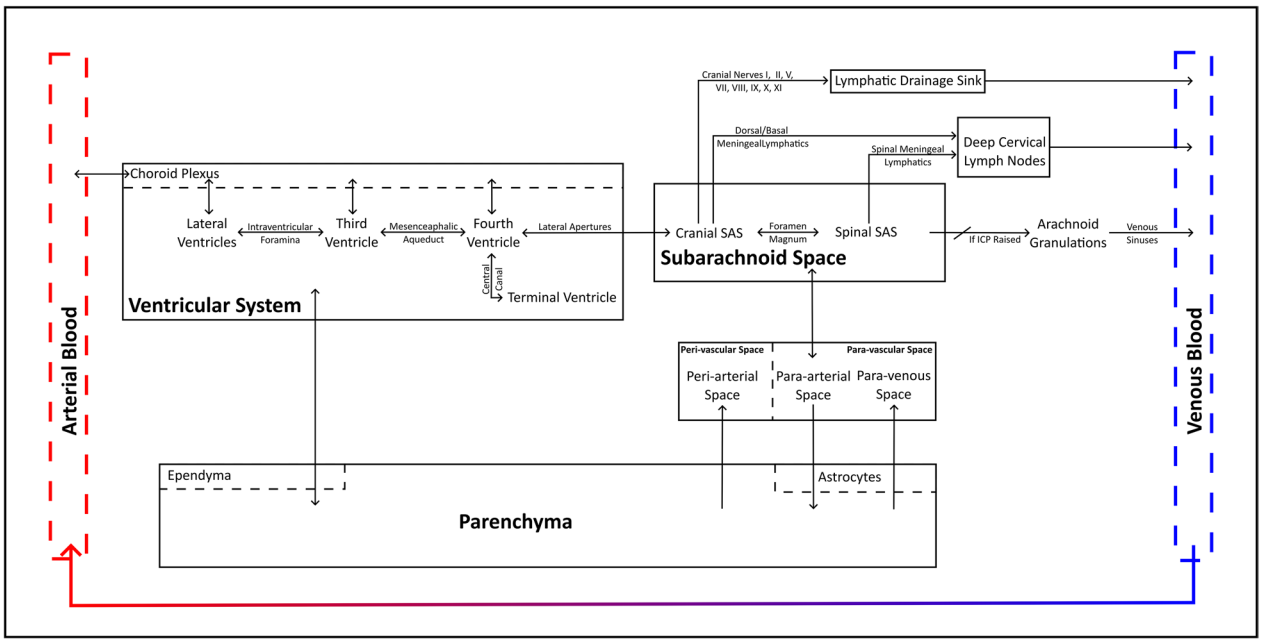

Fig. 8 A system diagram of the cerebrospinal fluid flow system, arrows indicate flow directionality

of the sleep-cycle contribute to fluid clearance uniquely. They found that sleep dependent changes in the vascular dynamics of pial arteries and penetrating arterioles mirrored changes in the size of the para-vascular spaces, and that these changes likely significantly enhance solute clearance from the brain [124].

Posture

It has been proposed that body position can influence CSF drainage. Lee et al. quantified CSF and interstitial fluid exchange during the supine, prone, and lateral positions in rodents. They found the most efficient clearance in the lateral position, with the least occurring in the prone posture. As the lateral position is the preferred sleeping position, they propose that this evolved to optimise waste clearance in sleep and that posture plays an implicit role in increased CSF clearance in sleep [125].

Klarica et al. investigated CSF pressure gradients in cats using an experimental model [126]. Anesthetised cats were fixed in sternal recumbency relative to an adjustable platform, which was rotated between 90 (upright) and 270 (head-down) degrees, including 0 degrees (horizontal). Pressure transducers were connected via cannulas to the lateral ventricle and lumbar SAS. The fore- and hindlimbs were outstretched. They found that, in an upright position, CSF pressure it the foramen magnum was at near atmospheric levels, and as such the pressure in the cranial vault was negative (subatmospheric). In the lumbar spine, a pressure gradient was observed proportional to the vertical distance to the foramen magnum, narrowing the cervical SAS, causing the dura to adhere to the spinal cord, and expanding the dural lumbar sac. Conversely, when in a horizontal position, pressures inside the lateral ventricles and lumbar SAS where similar [126]. Similar observations have been made in humans [127]. In alligators, an investigation by Taylor et al. found that posture influenced the relative contribution to CSF pressure pulsation between the cardiac and ventilatory systems, with cardiac dominating in head-down tilt, and ventilatory in head-up tilt. This relationship applied to both the cranial and spinal CSF pressure [41]; investigation into CSF pressure gradients in the dog remain absent.

Several studies have examined the impact of postural changes on CSF flow in humans. Alperin et al. observed CSF flow in the cervical SAS during horizontal and upright position, finding a reduction in CSF oscillatory volume, and increased intracranial compliance when upright. A reduction in intracranial volume when upright leads to increased compliance, and reduced cranial blood and CSF volume [128]. A subsequent study found that the spinal canal contributed more to the overall cranio-spinal compliance when in the supine position, while the cranium provided a greater proportion when upright. They proposed that the spinal canal therefore plays a role in buffering intracranial pressure during postural change. Additionally, it was observed that the lower-pressure CSF system was more sensitive to postural change that the relatively higher-pressure vascular system [129]. In another study, Muccio et al. used MRI to investigate the effect of

postural change in humans, finding greater CSF flow oscillation during the supine position compared to upright, and thus potentially greater CSF exchange. This change was driven by increased diastolic flow velocity, and systolic phase duration when supine [130].

Some studies on locomotion in reptiles have revealed that dynamic changes in posture significantly influence CSF flow dynamics [131, 132]. However, the significant anatomical and functional differences between mammals, such as dogs, and alligators prevent direct comparison.

Ageing and hypertension

Studies have found that ageing is associated with a decline in CSF influx. In mice, aging is related to a decline in drainage towards the lymphatic system, in addition to changes in the integrity of meningeal lymphatic vessels resulting in reduced functionality. Additionally, aging is associated with brain atrophy with ventricular and SAS enlargement. As such, CSF turnover is hypothesised to decrease [133]. Additionally, hypertension has been associated with variation in vascular elasticity, inhibiting the arterial wall motion that is hypothesised to drive para-vascular CSF flow [134].

Brachycephaly

The cranial index is an anthropometric measure to describe the ratio between the widest interzygomatic distance and inion-to-prosthion distance of the skull. This parameter is used in veterinary research to categorise the cranial morphology of dogs and cats. In this system there exist three major categories: dolichocephaly, mesaticephaly (mesocephaly) and brachycephaly, bounded by cranial indices of 0.39, 0.52, and 0.81 respectively [10]. However, other attempts have been made to numerically define different skull morphologies, Regodón et al. postulate that characteristic shortening of the cranium observed in brachycephalic dog breeds indicates compensatory perpendicular development of the cranium relative to the facial axis. As such, they define brachycephaly as a craniofacial angle between 9 and 14 degrees [135]. Alternatively, brachycephaly has been defined as the ratio between the length of the cranium, and the length of the skull [136]. More broadly, brachycephaly can be characterised by a rounded head, and shortened muzzle, in more extreme cases this can result in a dorsally rotated snout [137]. The characteristic conformational changes of the skull associated with canine brachycephaly are illustrated in Fig. 9.

The morphological diversity displayed by each distinct category is a result of generations of human artificial selection in breeding [138]. During normal foetal development, the bones of the cranium are initially separated and slowly ossify at a rate regulated by a mechanosensory system within the dura. Through this system, the skull develops in response to the increasing brain mass, with the ultimate shape of the skull being dependent on the growth of the cranial sutures [2]. Craniosynostosis is a developmental deformity of the infant skull due to the

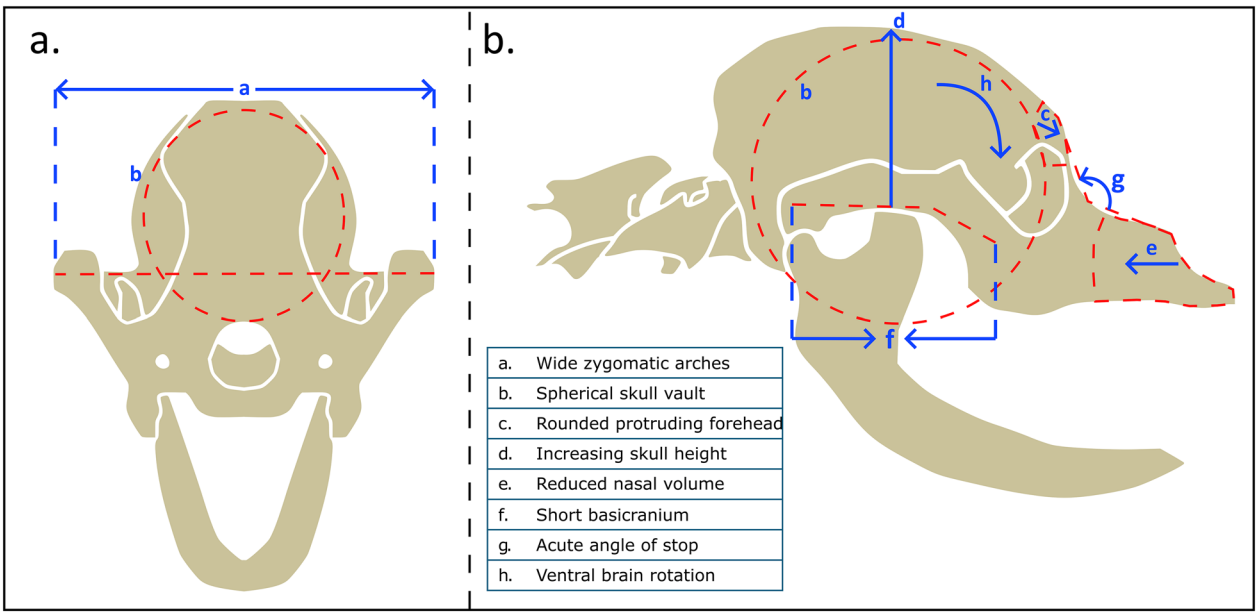

Fig. 9 Conformational changes to the skull associated with brachycephaly in the **a** transverse plane. **b** Sagittal plane. Blue arrows indicate the direction of tissue movement with increasing disease severity

premature ossification of cranial sutures. The resultant shape of the skull is defined by Virchow's law which states that compensatory growth occurs parallel to the prematurely closed suture as the skull cannot expand perpendicularly [139]. The aforementioned morphological categories are cases of complex craniosynostosis in which the premature fusion of multiple sutures gives rise to the characteristic cranial morphology. As craniosynostosis is congenital, these characteristics are then inherited in breeding.

Brachycephaly in dogs is a result of artificial selection for neotenous characteristics such as a broad domed forehead, flattened muzzle, and a rounded, less angular face [140]. In the context of craniosynostosis, brachycephaly is associated with the premature closure of the skull-base sutures predominately the basispheno-presphenoid and spheno-occipital synchondroses [141], giving rise to calvarial doming, however brachycephaly can present with the premature closure of other cranial sutures depending on the severity. Additionally, brachycephalic dogs present with wide zygomatic arches and rostro-caudal shortening of the muzzle, in some flat faced breeds the snout may be angled upwards (airorhynchy) rostrally and the junction between the frontal and nasal bone (stop) becomes increasingly acute (craniofacial hypoplasia) [137, 142].

There is an increasing body of evidence to suggest that the lymphatic system represents a major efflux route for CSF especially via the olfactory nerve, see section: Lymphatic Efflux. This pathway encircles the olfactory nerve fibres which penetrate the cribriform plate of the ethmoid bone within the rostral cranial fossa. A study by Sokołowski et al. used computed tomography morphometric analysis of the rostral cranial fossa to determine the ratio between the rostral cranial fossa and cranial cavity across different dog breeds spanning the three major conformational categories. They found that a reduced rostral cranial fossa volume was present in brachycephalic dogs and hypothesises that this may impede CSF efflux through the cribriform plate due to a reduction in the lymphatic vessel surface area [143]. Additionally, further conformational changes including craniofacial hypoplasia and airorhynchy, associated with flat faced brachycephaly in dogs, may impede efflux via the olfactory nerve route due to a reduction in the nasal mucosa [2].

In addition to the olfactory nerve route, it is likely that other lymphatic efflux pathways are similarly inhibited by brachycephaly. Brachycephalic dogs present with stenosis of the jugular foramen [144], which facilitates the passage of the basal meningeal lymphatic efflux via the sigmoid sinus and cranial nerve routes (IX, X, and XI). As such, it is probable that a reduction in the jugular foramen volume associated with brachycephaly will result in impaired CSF efflux through this region [2]. The structural changes associated with brachycephaly (reduced rostral cranial fossa volume, craniofacial hypoplasia, airorhynchy, and jugular foramen stenosis) collectively impair key CSF efflux pathways, likely disrupting intracranial fluid homeostasis, and predisposing brachycephalic breeds to CSF flow disorders. As such, these breeds provide a unique opportunity to explore conditions analogous to comparable human disorders characterized by craniosynostosis, such as Chiari-like malformation and syringomyelia. The effects of brachycephaly on the fluid flow system are indicated in Fig. 11.

Canine Chiari malformation

Canine Chiari(-like) malformation is a complex congenital condition associated with pain; however, the definition is contentious. In humans, Chiari malformation is a neurological herniation presenting with a reduced posterior fossa and caudal descent of the brainstem and cerebellum, this definition is categorised further into types depending on the presentation of the condition. This modern description is a deviation from the original description of the condition [145, 146]. In 2006 it was determined that the veterinary condition should be named Chiari-like malformation to distinguish it from the human condition as dogs do not possess cerebellar tonsils, and the severity of the condition is independent of cerebellar herniation severity [147]. Additionally, Chiari-like malformation was defined as "decreased caudal fossa volume with caudal descent of the cerebellum, and often the brainstem, into or through the foramen magnum" [146], however some authors support a broader definition. Knowler et al. define Chiari-like malformation as "a malformation of the skull and cranio-cervical junction which compromises the neural parenchyma to cause pain and/or disrupt CSF circulation which can result in syringomyelia" [147].

Brachycephalic dogs are predisposed to Chiari-like malformation; premature cranial suture closure results in a decreased skull length leading to overcrowding of the brain parenchyma leading to caudal displacement of the brainstem and cerebellum. Overcrowding is exacerbated by a reduced caudal cranial fossa [148]. Chiari-like malformation related pain is further associated with increasingly severe brachycephaly. Rusbridge and Knowler et al. detail the features of Chiari-like malformation related pain, shown in Fig. 10 [147, 149]. The regions affected by Chiari-like malformation are summarised in Fig. 11.

Syringomyelia

Syringomyelia is a condition in which a fluid-filled cavity (syrinx) forms within the spinal cord, the composition of this fluid is understood to be similar to CSF [1]. The United Kingdom Kennel Club (KC) and British

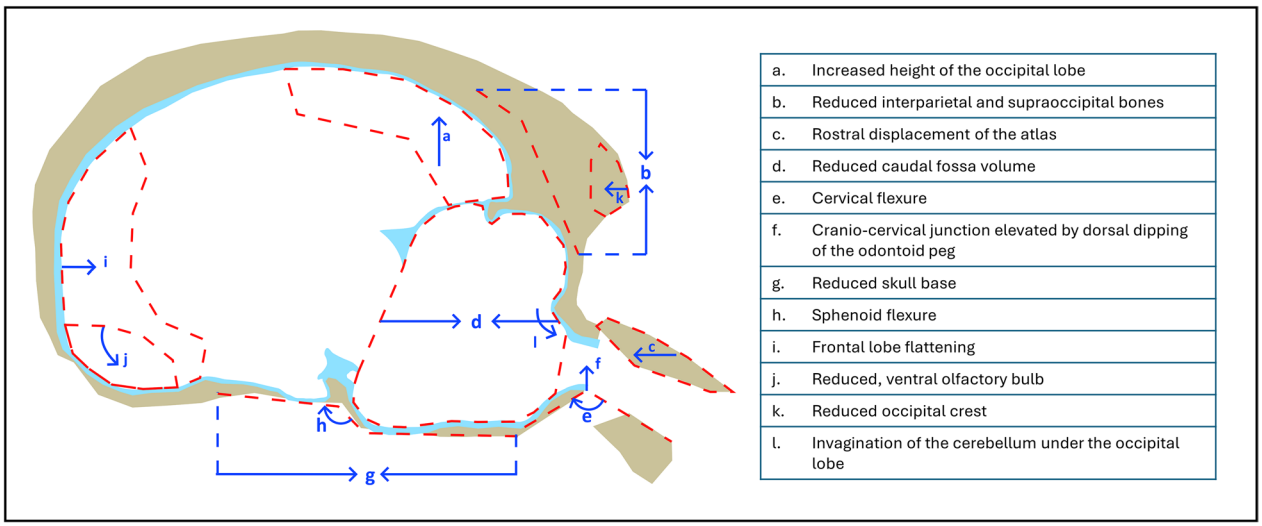

a.	Increased height of the occipital lobe
b.	Reduced interparietal and supraoccipital bones
c.	Rostral displacement of the atlas
d.	Reduced caudal fossa volume
e.	Cervical flexure
f.	Cranio-cervical junction elevated by dorsal dipping of the odontoid peg
g.	Reduced skull base
h.	Sphenoid flexure
i.	Frontal lobe flattening
j.	Reduced, ventral olfactory bulb
k.	Reduced occipital crest
l.	Invagination of the cerebellum under the occipital lobe

Fig. 10 Conformational changes associated with Chiari-like malformation in the sagittal plane. Blue arrows indicate the direction of tissue movement with increasing disease severity

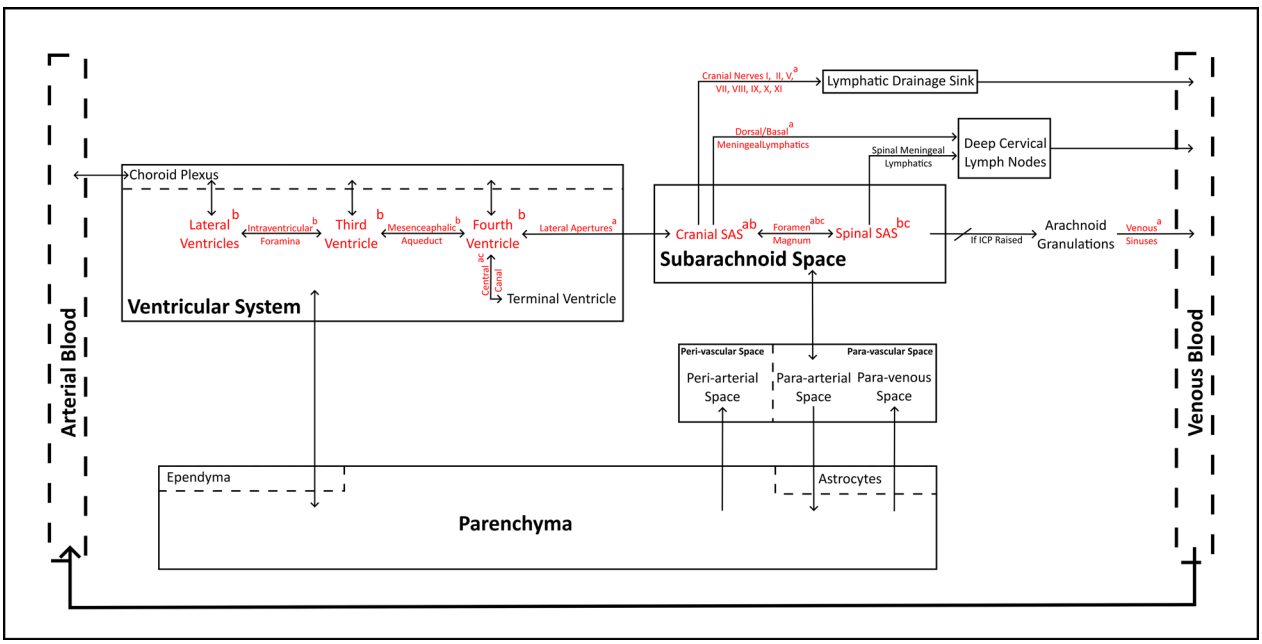

Fig. 11 Regions of the cerebrospinal fluid flow system affected by **a** Brachycephaly, **b** Chiari(-like) malformation, and **c** Syringomyelia. Red indicates sites characteristically affected fluid flow, and consequently key regions of interest for modelling disease states

Veterinary Association (BVA) define syringomyelia with respect to both the age of the patient, and transverse width of the cavitation.

The aetiology of syringomyelia is diverse and poorly defined. In veterinary medicine syringomyelia is most commonly associated with Chiari-like malformation [2]. Driver et al. found that more severe overcrowding of the cranial caudal fossa is positively correlated with syringomyelia, and that caudal cranial fossa parenchyma volume and syrinx width and ventricle size are also positively correlated indicating that syringomyelia occurs as a result of altered CSF dynamics [150]. However, Couturier et al. failed to identify any correlation between cranial caudal fossa volume and syringomyelia in a population of Chiari-like malformation affected dogs, they instead found that the only difference between dogs with

or without syringomyelia was age; dogs with Chiari-like malformation and syringomyelia were statistically older likely owing to the progressive nature of syringomyelia [151]. In addition to overcrowding, some studies have found that impaired venous drainage is associated with syringomyelia [144, 152–155]. The percentage of the caudal cranial fossa occupied by the venous sinuses is significantly smaller in Cavelier King Charles Spaniels with syringomyelia [152], and dogs affected with syringomyelia present with significantly smaller jugular foramina volumes [144]. Abnormalities at the cranio-cervical junction have also been associated with syringomyelia. A more caudally located brainstem is associated with the development of syringomyelia [153], furthermore, there is a relationship between dorsal compressive lesions at the atlantoaxial junction, and syringomyelia with the severity being related to the compression index [154]. A 2016 study found that there is a significant relationship between atlanto-occipital overlapping, and syringomyelia [155]. Rusbridge and Knowler propose that the aetiology of syringomyelia is multifactorial, developing due to a combination of: reduced CSF absorption, reduced venous drainage, altered neuroparenchymal compliance, reduced CSF flow through the cranio-cervical junction or lateral apertures of the fourth ventricle [2].

The mechanism through which syringomyelia develops is a matter of debate, currently the most accepted theory centres around a delay between the peak arterial pressure and peak CSF pressure pulses [2]. The para-vascular space is dynamic, changing size throughout the cardiac cycle, due to variation in the diameter of penetrating arterioles. This space is at its widest when the arterial pressure is at its minimum and is narrowest at peak arterial pressure. If the CSF pressure waveform is out of phase with the arterial pressure waveform such that peak CSF pressure occurs prior to peak arterial pressure, flow of CSF into the spinal cord is favoured over outflow into the SAS. In this case, the para-vascular space acts like a leaky one-way valve, resulting in preferential flow into the spinal cord [156]. This mechanism is largely based on the results of computational modelling studies and is as such limited by the simplifying assumptions inherent in such studies. More recent studies by the same research group raise doubts about the viability of this hypothesis for physiologically plausible range of parameters. Both Lloyd et al. and Martinac et al. observed that the leaky valve can operate effectively only if the radial displacement magnitude of the penetrating artery wall is up to one order of magnitude higher than experimentally observed values [82, 157, 158]. Furthermore, Martinac et al. demonstrated that physiologically implausible time delays between blood and CSF pulses were required for the leaky valve to operate, even when arterial displacement is maintained at unrealistically high levels [158].

For a discussion of the theories of syringomyelia pathogenesis see [159]. In the case that a syrinx is already present in the spinal cord, the syrinx may increase in size through the "slosh" mechanism prosed by Williams [160], and further investigated by Cirovic and Rusbridge, and Bertram and Heil [46, 161]. Epidural venous distention during Valsalva manoeuvre initiates the movement of CSF in the spinal SAS, compressing the syrinx at one end. This generates movement of fluid within the syrinx towards the other end of the cavity, stressing the spinal cord tissue and resulting in enlargement of the syrinx [46]. The CSF flow systems affected by syringomyelia are summarised in Fig. 11.

Incidence of Chiari-like malformation and syringomyelia in dogs

In humans, the prevalence of craniosynostosis, Chiari malformation, and syringomyelia are low. Craniosynostosis affects approximately 0.05% of live births [162], whereas type 1 Chiari malformation affects around 0.1% of the population, of which 30% display concurrent syringomyelia [163]. In Italy, Ciaramitaro et al. found the prevalence of Chiari malformation and syringomyelia to be 0.008% and 0.005% respectively [164], whereas in the Russian Federation, Klimov et al. found the incidence of syringomyelia to be around 0.01%, potentially owing to a familial predisposition in the Tartar population [165]. Comparatively, brachycephalic dogs have significantly higher reported incidence. The Cavalier King Charles spaniel has an estimated incidence of 77–100% for Chiari-like malformation, and 15–79% for syringomyelia, however, the incidence reported in literature varies significantly depending on the population studied (veterinary clinics, breeding populations, etc.), exclusion/inclusion criteria (age, clinical signs, etc.), and diagnostic criteria (MRI findings, owner reported, etc.). Similarly, Griffon Bruxellois have estimated incidence of 61–80% and 45–74% for Chiari-like malformation and syringomyelia respectively. Complete incidence data for Chiari-like malformation and syringomyelia in brachycephalic dog breeds are provided in the supplementary material [see Additional File 1]. It is worth noting that the statistical power of these prevalence studies is low, however, they demonstrate a significant increase in prevalence compared to humans, and an increased incidence with age. Therefore, modelling Chiari-malformation and syringomyelia in the context of brachycephalic dogs provides access to larger datasets than solely analysing the human condition.

Conclusion

The CSF flow system plays an essential role in maintaining neural homeostasis by facilitating waste clearance and regulating intracranial pressure. Disruptions in CSF flow can lead to severe neurological conditions,

as evidenced by the prevalence of Chiari(-like) malformation and syringomyelia in both humans and certain brachycephalic dog breeds. Brachycephalic dogs, due to their predisposition to CSF-related disorders, offer valuable insights into the mechanisms and potential therapeutic targets for similar human pathologies. This review has presented a complete synthesis of the contemporary understanding of CSF flow, collating evidence from human, rodent, and mammalian studies. This literature has been used to generate a CSF flow system, which can be applied to analyse neurological conditions to improve our understanding of CSF flow dynamics and to develop more effective models for conditions arising from CSF dysregulation.

Abbreviations

BVA	British Veterinary Association
CSF	Cerebrospinal fluid
IPAD	Intramural periarterial drainage
KC	Kennel Club
MRI	Magnetic Resonance Imaging
SAS	Subarachnoid space

Supplementary Information

The online version contains supplementary material available at https://doi.org/10.1186/s12987-025-00636-x.

Additional file 1.

Acknowledgements
The authors are grateful to the Hannah Hasty Memorial Fund for contributing to funding this publication.

Author contributions
RJ, CR, SC conceived this review. RJ wrote the manuscript, CR and SC provided editorial feedback. All authors reviewed the manuscript.

Funding
University of Surrey provided support in the form of salaries, materials, and access to software. The funders had no role in the decision to publish, or preparation of the manuscript.

Availability of data and materials
No datasets were generated or analysed during the current study.

Declarations

Ethics approval and consent to participate
Not applicable.

Consent for publication
Not applicable.

Competing interests
The authors declare no competing interests.

Received: 23 October 2024 Accepted: 19 February 2025
Published online: 10 March 2025

References

1. Brodbelt A. The biochemistry of syringomyelia. In: Flint G, Rusbridge C, editors. Syringomyelia: a disorder of CSF circulation. Berlin, Heidelberg: Springer Berlin Heidelberg; 2014. p. 261–78. https://doi.org/10.1007/978-3-642-13706-8_17.
2. Rusbridge C, Knowler P. The need for head space: brachycephaly and cerebrospinal fluid disorders. Life. 2021;11(2):139.
3. Matsumae M, Kuroda K, Yatsushiro S, Hirayama A, Hayashi N, Takizawa K, et al. Changing the currently held concept of cerebrospinal fluid dynamics based on shared findings of cerebrospinal fluid motion in the cranial cavity using various types of magnetic resonance imaging techniques. Neurol Med Chir (Tokyo). 2019;59(4):133–46.
4. Brinker T, Stopa E, Morrison J, Klinge P. A new look at cerebrospinal fluid circulation. Fluids Barriers CNS. 2014;11(1):10.
5. Christen MA, Schweizer-Gorgas D, Richter H, Joerger FB, Dennler M. Quantification of cerebrospinal fluid flow in dogs by cardiac-gated phase-contrast magnetic resonance imaging. J Vet Intern Med. 2021;35(1):333–40.
6. Mantovani G, Menegatti M, Scerrati A, Cavallo MA, De Bonis P. Controversies and misconceptions related to cerebrospinal fluid circulation: a review of the literature from the historical pioneers' theories to current models. Biomed Res Int. 2018;26(2018):1–7.
7. Agarwal N, Lewis LD, Hirschler L, Rivera LR, Naganawa S, Levendovszky SR, et al. Current understanding of the anatomy, physiology, and magnetic resonance imaging of neurofluids: update from the 2022 "ISMRM Imaging Neurofluids Study group" Workshop in Rome. J Magn Reson Imaging. 2024;59(2):431–49.
8. Marín-García P, González-Soriano J, Martinez-Sainz P, Contreras-Rodríguez J, Del C-G, Rodríguez-Veiga E. Spinal cord central canal of the German shepherd dog: morphological, histological, and ultrastructural considerations. J Morphol. 1995;224(2):205–12.
9. Sakata M, Yashika K, Hashimoto PH. Caudal aperture of the central canal at the filum terminale in primates. Kaibogaku Zasshi. 1993;68(2):213–9.
10. Evans HE, de Lahunta A. Miller's anatomy of the dog. 4th ed. St. Louis, MO: Elsevier; 2013.
11. James AE, Flor WJ, Novak GR, Strecker EP, Burns B. Evaluation of the central canal of the spinal cord in experimentally induced hydrocephalus. J Neurosurg. 1978;48(6):970–4.
12. Milhorat TH, Kotzen RM, Anzil AP. Stenosis of central canal of spinal cord in man: incidence and pathological findings in 232 autopsy cases. J Neurosurg. 1994;80(4):716–22.
13. Hashizume Y, Yasui K, Yoshida M. Age-related morphological change of the central canal of the human spinal cord and the mechanism of syrinx formation in syringomyelia and hydromyelia. In: Syringomyelia. Tokyo: Springer Japan; 2001. p. 31–9.
14. Anagnostakou V, Epshtein M, Peker A, Puri AS, Singh J, Ughi GJ, et al. New frontiers in intracranial imaging with HF-OCT: Ex vivo human cerebrovasculature evaluation and in vivo intracranial arteries dynamic visualization. Front Photon. 2022;1:3.
15. Eide PK, Ringstad G. Functional analysis of the human perivascular subarachnoid space. Nat Commun. 2024;15(1):2001.
16. Møllgård K, Beinlich FRM, Kusk P, Miyakoshi LM, Delle C, Plá V, et al. A mesothelium divides the subarachnoid space into functional compartments. Science (1979). 2023;379(6627):84–8.
17. Plá V, Bitsika S, Giannetto MJ, Ladron-de-Guevara A, Gahn-Martinez D, Mori Y, et al. Structural characterization of SLYM—a 4th meningeal membrane. Fluids Barriers CNS. 2023;20(1):93.
18. Neuhuber W. An, "outer subarachnoid space": fact or artefact? A commentary on "Structural characterization of SLYM– a 4th meningeal membrane" fluids and barriers of the CNS (2023) 20:93 by V. Plá et al. Fluids Barriers CNS. 2024;21(1):48.
19. Plá V, Bitsika S, Giannetto MJ, Ladron-de-Guevara A, Gahn-Martinez D, Mori Y, et al. In response to "An 'outer subarachnoid space': fact or artefact? A commentary on 'Structural characterization of SLYM: a 4th meningeal membrane' fluids and barriers of the CNS (2023) 20:93 by V. Plá et al. Fluids Barriers CNS. 2024;21(1):49.
20. Siegenthaler J, Betsholtz C. Commentary on "Structural characterization of SLYM—a 4th meningeal membrane." Fluids Barriers CNS. 2024;21(1):69.
21. Plá V, Bitsika S, Giannetto MJ, Ladrón-de-Guevara A, Gahn-Martinez D, Mori Y, et al. Response to Commentary on "Structural characterization of

SLYM—a 4th meningeal membrane" by Julie Siegenthaler and Christer Betsholtz. Fluids Barriers CNS. 2024;21(1):70.
22. Kelley DH, Thomas JH. Cerebrospinal fluid flow. Annu Rev Fluid Mech. 2023;55(1):237–64.
23. Coben LA. Absence of a foramen of magendie in the dog, cat, rabbit, and goat. Arch Neurol. 1967;16(5):524–8.
24. Faubel R, Westendorf C, Bodenschatz E, Eichele G. Cilia-based flow network in the brain ventricles. Science (1979). 2016;353(6295):176–8.
25. Olstad EW, Ringers C, Hansen JN, Wens A, Brandt C, Wachten D, et al. Ciliary beating compartmentalizes cerebrospinal fluid flow in the brain and regulates ventricular development. Curr Biol. 2019;29(2):229-241.e6.
26. Thouvenin O, Keiser L, Cantaut-Belarif Y, Carbo-Tano M, Verweij F, Jurisch-Yaksi N, et al. Origin and role of the cerebrospinal fluid bidirectional flow in the central canal. Elife. 2020;9:9.
27. Siyahhan B, Knobloch V, de Zélicourt D, Asgari M, Schmid Daners M, Poulikakos D, et al. Flow induced by ependymal cilia dominates near-wall cerebrospinal fluid dynamics in the lateral ventricles. J R Soc Interface. 2014;11(94):20131189.
28. Chen L, Beckett A, Verma A, Feinberg DA. Dynamics of respiratory and cardiac CSF motion revealed with real-time simultaneous multi-slice EPI velocity phase contrast imaging. Neuroimage. 2015;122:281–7.
29. Wichmann TO, Damkier HH, Pedersen M. A brief overview of the cerebrospinal fluid system and its implications for brain and spinal cord diseases. Front Hum Neurosci. 2022;21:15.
30. Takizawa K, Matsumae M, Sunohara S, Yatsushiro S, Kuroda K. Characterization of cardiac- and respiratory-driven cerebrospinal fluid motion based on asynchronous phase-contrast magnetic resonance imaging in volunteers. Fluids Barriers CNS. 2017;14(1):25.
31. Toro EF, Celant M, Zhang Q, Contarino C, Agarwal N, Linninger A, et al. Cerebrospinal fluid dynamics coupled to the global circulation in holistic setting: Mathematical models, numerical methods and applications. Int J Numer Method Biomed Eng. 2022. https://doi.org/10.1002/cnm.3532.
32. Mohsenian S, Ibrahimy A, Al Samman MMF, Oshinski JN, Bhadelia RA, Barrow DL, et al. Association between resistance to cerebrospinal fluid flow and cardiac-induced brain tissue motion for Chiari malformation type I. Neuroradiology. 2023;65(10):1535–43.
33. Zhu DC, Xenos M, Linninger AA, Penn RD. Dynamics of lateral ventricle and cerebrospinal fluid in normal and hydrocephalic brains. J Magn Reson Imaging. 2006;24(4):756–70.
34. Feinberg DA, Mark AS. Human brain motion and cerebrospinal fluid circulation demonstrated with MR velocity imaging. Radiology. 1987;163(3):793–9.
35. Bradley WG. CSF flow in the brain in the context of normal pressure hydrocephalus. Am J Neuroradiol. 2015;36(5):831–8.
36. Alperin NJ, Lee SH, Loth F, Raksin PB, Lichtor T. MR-intracranial pressure (ICP): a method to measure intracranial elastance and pressure noninvasively by means of MR imaging: baboon and human study. Radiology. 2000;217(3):877–85.
37. Gutiérrez-Montes C, Coenen W, Vidorreta M, Sincomb S, Martínez-Bazán C, Sánchez AL, et al. Effect of normal breathing on the movement of CSF in the spinal subarachnoid space. Am J Neuroradiol. 2022;43(9):1369–74.
38. Aktas G, Kollmeier JM, Joseph AA, Merboldt KD, Ludwig HC, Gärtner J, et al. Spinal CSF flow in response to forced thoracic and abdominal respiration. Fluids Barriers CNS. 2019;16(1):10.
39. Yamada S, Miyazaki M, Yamashita Y, Ouyang C, Yui M, Nakahashi M, et al. Influence of respiration on cerebrospinal fluid movement using magnetic resonance spin labeling. Fluids Barriers CNS. 2013;10(1):36.
40. Lloyd RA, Butler JE, Gandevia SC, Ball IK, Toson B, Stoodley MA, et al. Respiratory cerebrospinal fluid flow is driven by the thoracic and lumbar spinal pressures. J Physiol. 2020;598(24):5789–805.
41. Taylor Z, English C, Cramberg M, Young BA. The influence of spinal venous blood pressure on cerebrospinal fluid pressure. Sci Rep. 2023;13(1):20989.
42. Spijkerman JM, Geurts LJ, Siero JCW, Hendrikse J, Luijten PR, Zwanenburg JJM. Phase contrast MRI measurements of net cerebrospinal fluid flow through the cerebral aqueduct are confounded by respiration. J Magn Reson Imaging. 2019;49(2):433–44.
43. Yatsushiro S, Sunohara S, Tokushima T, Takizawa K, Matsumae M, Atsumi H, et al. Characterization of cardiac- and respiratory-driven cerebrospinal fluid motions using a correlation mapping technique based on asynchronous two-dimensional phase contrast MR imaging. Magn Reson Med Sci. 2021;20(4):20200085.
44. Williams B. Cerebrospinal fluid pressure changes in response to coughing. Brain. 1976;99(2):331–46.
45. Martin BA, Loth F. The influence of coughing on cerebrospinal fluid pressure in an in vitro syringomyelia model with spinal subarachnoid space stenosis. Cerebrospinal Fluid Res. 2009;6(1):17.
46. Cirovic S, Rusbridge C. Slosh simulation in a computer model of canine syringomyelia. Life. 2021;11(10):1083.
47. Phillips EL, Donofrio PD. Autonomic disorders. In: Encyclopedia of Neuroscience. Elsevier; 2009. p. 799–808. https://doi.org/10.1016/B978-008045046-9.00628-8.
48. Bhadelia RA, Madan N, Zhao Y, Wagshul ME, Heilman C, Butler JP, et al. Physiology-based MR imaging assessment of CSF flow at the foramen magnum with a Valsalva Maneuver. Am J Neuroradiol. 2013;34(9):1857–62.
49. MacAulay N, Keep RF, Zeuthen T. Cerebrospinal fluid production by the choroid plexus: a century of barrier research revisited. Fluids Barriers CNS. 2022;19(1):26.
50. Damkier HH, Brown PD, Praetorius J. Cerebrospinal fluid secretion by the choroid plexus. Physiol Rev. 2013;93(4):1847–92.
51. Bajda J, Pitla N, Gorantla VR. Bulat-Klarica-Oreskovic hypothesis: a comprehensive review. Cureus. 2023. https://doi.org/10.7759/cureus.45821.
52. Orešković D, Klarica M. The formation of cerebrospinal fluid: nearly a hundred years of interpretations and misinterpretations. Brain Res Rev. 2010;64(2):241–62.
53. Spector R, Keep RF, Robert Snodgrass S, Smith QR, Johanson CE. A balanced view of choroid plexus structure and function: focus on adult humans. Exp Neurol. 2015;267:78–86.
54. Orešković D, Radoš M, Klarica M. Role of choroid plexus in cerebrospinal fluid hydrodynamics. Neuroscience. 2017;354:69–87.
55. Keep RF, Barrand MA, Hladky SB. Comment on "Role of choroid plexus in cerebrospinal fluid hydrodynamics." Neuroscience. 2018;380:164.
56. Orešković D, Radoš M, Klarica M. Reply to comment on "Role of choroid plexus in cerebrospinal fluid hydrodynamics." Neuroscience. 2018;380:165.
57. Hladky SB, Barrand MA. Mechanisms of fluid movement into, through and out of the brain: evaluation of the evidence. Fluids Barriers CNS. 2014;11(1):26.
58. Hladky SB, Barrand MA. Regulation of brain fluid volumes and pressures: basic principles, intracranial hypertension, ventriculomegaly and hydrocephalus. Fluids Barriers CNS. 2024;21(1):57.
59. Gomez DG, Potts DG. The lateral, third, and fourth ventricle choroid plexus of the dog: a structural and ultrastructural study. Ann Neurol. 1981;10(4):333–40.
60. Bedussi B, van der Wel NN, de Vos J, van Veen H, Siebes M, VanBavel E, et al. Paravascular channels, cisterns, and the subarachnoid space in the rat brain: a single compartment with preferential pathways. J Cereb Blood Flow Metab. 2017;37(4):1374–85.
61. Durand-Fardel M. Traite du ramollissement du cerveau. Paris: Bailliere; 1843.
62. Virchow R. Ueber die Erweiterung kleinerer Gefäfse. Virchows Arch. 1851;3(3):427–62.
63. Robin CP. Recherches sur quelques particularites de la structure des capillaires de l'encephale. J Physiol Homme Animaux. 1859;2:537.
64. Weed LH. Studies on cerebro-spinal fluid. No. IV: the dual source of cerebro-spinal fluid. J Med Res. 1914;31(1):93–11811.
65. Leonhardt H, Desaga U. Recent observations on ependyma and subependymal basement membranes. Acta Neurochir (Wien). 1975;31(3–4):153–9.
66. Cserr HF, Cooper DN, Milhorat TH. Flow of cerebral interstitial fluid as indicated by the removal of extracellular markers from rat caudate nucleus. Exp Eye Res. 1977;25:461–73.
67. Hladky SB, Barrand MA. The glymphatic hypothesis: the theory and the evidence. Fluids Barriers CNS. 2022;19(1):9.
68. Rennels ML, Gregory TF, Blaumanis OR, Fujimoto K, Grady PA. Evidence for a 'Paravascular' fluid circulation in the mammalian central nervous

system, provided by the rapid distribution of tracer protein throughout the brain from the subarachnoid space. Brain Res. 1985;326(1):47–63.
69. Rennels ML, Blaumanis OR, Grady PA. Rapid solute transport throughout the brain via paravascular fluid pathways. Adv Neurol. 1990;52:431–9.
70. Iliff JJ, Wang M, Liao Y, Plogg BA, Peng W, Gundersen GA, et al. A paravascular pathway facilitates CSF flow through the brain parenchyma and the clearance of interstitial solutes, including amyloid β. Sci Transl Med. 2012;4(147).
71. Weller RO, Subash M, Preston SD, Mazanti I, Carare RO. SYMPOSIUM: clearance of Aβ from the brain in Alzheimer's disease: perivascular drainage of amyloid-β peptides from the brain and its failure in cerebral amyloid angiopathy and Alzheimer's disease. Brain Pathol. 2008;18(2):253–66.
72. Wardlaw JM, Benveniste H, Nedergaard M, Zlokovic BV, Mestre H, Lee H, et al. Perivascular spaces in the brain: anatomy, physiology and pathology. Nat Rev Neurol. 2020;16(3):137–53.
73. Mestre H, Hablitz LM, Xavier AL, Feng W, Zou W, Pu T, et al. Aquaporin-4-dependent glymphatic solute transport in the rodent brain. Elife. 2018;18:7.
74. Smith AJ, Akdemir G, Wadhwa M, Song D, Verkman AS. Application of fluorescent dextrans to the brain surface under constant pressure reveals AQP4-independent solute uptake. J Gen Physiol. 2021. https://doi.org/10.1085/jgp.202112898.
75. Wang MX, Ray L, Tanaka KF, Iliff JJ, Heys J. Varying perivascular astroglial endfoot dimensions along the vascular tree maintain perivascular-interstitial flux through the cortical mantle. Glia. 2021;69(3):715–28.
76. Min Rivas F, Liu J, Martell BC, Du T, Mestre H, Nedergaard M, et al. Surface periarterial spaces of the mouse brain are open, not porous. J R Soc Interface. 2020;17(172):20200593.
77. Tithof J, Kelley DH, Mestre H, Nedergaard M, Thomas JH. Hydraulic resistance of periarterial spaces in the brain. Fluids Barriers CNS. 2019;16(1):19.
78. Bedussi B, Almasian M, de Vos J, VanBavel E, Bakker EN. Paravascular spaces at the brain surface: Low resistance pathways for cerebrospinal fluid flow. J Cereb Blood Flow Metab. 2018;38(4):719–26.
79. Jessen NA, Munk ASF, Lundgaard I, Nedergaard M. The glymphatic system: a beginner's guide. Neurochem Res. 2015;40(12):2583–99.
80. Thomas JH. Fluid dynamics of cerebrospinal fluid flow in perivascular spaces. J R Soc Interface. 2019;16(159):20190572.
81. Ladrón-de-Guevara A, Shang JK, Nedergaard M, Kelley DH. Perivascular pumping in the mouse brain: Improved boundary conditions reconcile theory, simulation, and experiment. J Theor Biol. 2022;542: 111103.
82. Mestre H, Tithof J, Du T, Song W, Peng W, Sweeney AM, et al. Flow of cerebrospinal fluid is driven by arterial pulsations and is reduced in hypertension. Nat Commun. 2018;9(1):4878.
83. Gan Y, Holstein-Rønsbo S, Nedergaard M, Boster KAS, Thomas JH, Kelley DH. Perivascular pumping of cerebrospinal fluid in the brain with a valve mechanism. J R Soc Interface. 2023. https://doi.org/10.1098/rsif.2023.0288.
84. Kedarasetti RT, Drew PJ, Costanzo F. Arterial pulsations drive oscillatory flow of CSF but not directional pumping. Sci Rep. 2020;10(1):10102.
85. Raghunandan A, Ladron-de-Guevara A, Tithof J, Mestre H, Du T, Nedergaard M, et al. Bulk flow of cerebrospinal fluid observed in periarterial spaces is not an artifact of injection. Elife. 2021;9:10.
86. Li AM, Xu J. Cerebrospinal fluid-tissue exchange revealed by phase alternate labeling with null recovery MRI. Magn Reson Med. 2022;87(3):1207–17.
87. Casaca-Carreira J, Temel Y, Hescham SA, Jahanshahi A. Transependymal cerebrospinal fluid flow: opportunity for drug delivery? Mol Neurobiol. 2018;55(4):2780–8.
88. Yang PH, Almgren-Bell A, Gu H, Dowling AV, Pugazenthi S, Mackey K, et al. Etiology- and region-specific characteristics of transependymal cerebrospinal fluid flow. J Neurosurg Pediatr. 2022;30(4):437–47.
89. Strecker EP, James AE, Kelley JET, Merz T. Semiquantitative studies of transependymal albumin movement in communicating hydrocephalus. Radiology. 1974;111(2):341–6.
90. Sun Y, Liu E, Pei Y, Yao Q, Ma H, Mu Y, et al. The impairment of intramural periarterial drainage in brain after subarachnoid hemorrhage. Acta Neuropathol Commun. 2022;10(1):187.
91. van Veluw SJ, Hou SS, Calvo-Rodriguez M, Arbel-Ornath M, Snyder AC, Frosch MP, et al. Vasomotion as a driving force for paravascular clearance in the awake mouse brain. Neuron. 2020;105(3):549-561.e5.
92. Albargothy NJ, Johnston DA, MacGregor-Sharp M, Weller RO, Verma A, Hawkes CA, et al. Convective influx/glymphatic system: tracers injected into the CSF enter and leave the brain along separate periarterial basement membrane pathways. Acta Neuropathol. 2018;136(1):139–52.
93. Carare RO, Bernardes-Silva M, Newman TA, Page AM, Nicoll JAR, Perry VH, et al. Solutes, but not cells, drain from the brain parenchyma along basement membranes of capillaries and arteries: significance for cerebral amyloid angiopathy and neuroimmunology. Neuropathol Appl Neurobiol. 2008;34(2):131–44.
94. Aldea R, Weller RO, Wilcock DM, Carare RO, Richardson G. Cerebrovascular smooth muscle cells as the drivers of intramural periarterial drainage of the brain. Front Aging Neurosci. 2019;23:11.
95. Yoon JH, Jin H, Kim HJ, Hong SP, Yang MJ, Ahn JH, et al. Nasopharyngeal lymphatic plexus is a hub for cerebrospinal fluid drainage. Nature. 2024;625(7996):768–77.
96. Ma Q, Ineichen BV, Detmar M, Proulx ST. Outflow of cerebrospinal fluid is predominantly through lymphatic vessels and is reduced in aged mice. Nat Commun. 2017;8(1):1434.
97. Johnston M, Zakharov A, Papaiconomou C, Salmasi G, Armstrong D. Evidence of connections between cerebrospinal fluid and nasal lymphatic vessels in humans, non-human primates and other mammalian species. Cerebrospinal Fluid Res. 2004;1(1):2.
98. Kida S. Lymphatic drainage of CSF and ISF from the brain: recent concept and hypothesis. Rinsho Shinkeigaku. 2014;54(12):1187–9.
99. Decker Y, Krämer J, Xin L, Müller A, Scheller A, Fassbender K, et al. Magnetic resonance imaging of cerebrospinal fluid outflow after low-rate lateral ventricle infusion in mice. JCI Insight. 2022;7(3).
100. Chae J, Choi M, Choi J, Yoo SJ. The nasal lymphatic route of CSF outflow: implications for neurodegenerative disease diagnosis and monitoring. Anim Cells Syst (Seoul). 2024;28(1):45–54.
101. Liu H, Ni Z, Chen Y, Wang D, Qi Y, Zhang Q, et al. Olfactory route for cerebrospinal fluid drainage into the cervical lymphatic system in a rabbit experimental model. Neural Regen Res. 2012;7(10):766–71.
102. Walter BA, Valera VA, Takahashi S, Ushiki T. The olfactory route for cerebrospinal fluid drainage into the peripheral lymphatic system. Neuropathol Appl Neurobiol. 2006;32(4):388–96.
103. Zakharov A, Papaiconomou C, Johnston M. Lymphatic vessels gain access to cerebrospinal fluid through unique association with olfactory nerves. Lymphat Res Biol. 2004;2(3):139–46.
104. Lüdemann W, Berens von Rautenfeld D, Samii M, Brinker T. Ultrastructure of the cerebrospinal fluid outflow along the optic nerve into the lymphatic system. Child's Nervous Syst. 2005;21(2):96–103.
105. Sheng J, Li Q, Liu T, Wang X. Cerebrospinal fluid dynamics along the optic nerve. Front Neurol. 2022;15:13.
106. de la Motte DJ. Removal of horseradish peroxidase and fluorescein-labelled dextran from CSF spaces of rabbit optic nerve. A light and electron microscope study. Exp Eye Res. 1978;27(5):585–94.
107. Manzo RP, Gomez DG, Potts DG. Cerebrospinal fluid absorption in the rabbit: inner ear pathways. Acta Otolaryngol. 1990;109(5–6):389–96.
108. Lavrova AI, Postnikov EB. Barenblatt-like approach to transport processes in meningeal lymphatic vessel's dynamics. Eur Phys J Plus. 2021;136(5):486.
109. Maloveská M, Humeník F, Vikartovská Z, Hudáková N, Almášiová V, Krešáková L, et al. Brain fluid channels for metabolite removal. Physiol Res. 2022;2:199–208.
110. Papadopoulos Z, Herz J, Kipnis J. Meningeal lymphatics: from anatomy to central nervous system immune surveillance. J Immunol. 2020;204(2):286–93.
111. Miura M, Kato S, von Lündinghausen M. Lymphatic drainage of the cerebrospinal fluid from monkey spinal meninges with special reference to the distribution of the epidural lymphatics. Arch Histol Cytol. 1998;61(3):277–86.
112. Sokołowski W, Barszcz K, Kupczyńska M, Czubaj N, Skibniewski M, Purzyc H. Lymphatic drainage of cerebrospinal fluid in mammals—are arachnoid granulations the main route of cerebrospinal fluid outflow? Biologia (Bratisl). 2018;73(6):563–8.

113. Lee DS, Suh M, Sarker A, Choi Y. Brain Glymphatic/Lymphatic Imaging by MRI and PET. Nucl Med Mol Imaging. 2020;54(5):207–23.
114. Pollay M. The function and structure of the cerebrospinal fluid outflow system. Cerebrospinal Fluid Res. 2010;7(1):9.
115. de Lahunta A, Glass E, Kent M. Cerebrospinal fluid and hydrocephalus. In: de Lahunta's Veterinary Neuroanatomy and Clinical Neurology. Elsevier; 2021. p. 79–105.
116. Proulx ST. Cerebrospinal fluid outflow: a review of the historical and contemporary evidence for arachnoid villi, perineural routes, and dural lymphatics. Cell Mol Life Sci. 2021;78(6):2429–57.
117. Pollay M, Welch K. The function and structure of canine arachnoid villi. J Surg Res. 1962;2(5):307–11.
118. Radoš M, Živko M, Periša A, Orešković D, Klarica M. No arachnoid granulations—no problems: number, size, and distribution of arachnoid granulations from birth to 80 years of age. Front Aging Neurosci. 2021;1:13.
119. Schurr PH, McLaurin RL, Ingraham FD. Experimental studies on the circulation of the cerebrospinal fluid. J Neurosurg. 1953;10(5):515–25.
120. Eide PK, Valnes LM, Pripp AH, Mardal KA, Ringstad G. Delayed clearance of cerebrospinal fluid tracer from choroid plexus in idiopathic normal pressure hydrocephalus. J Cereb Blood Flow Metab. 2020;40(9):1849–58.
121. Czarniak N, Kamińska J, Matowicka-Karna J, Koper-Lenkiewicz O. Cerebrospinal fluid-basic concepts review. Biomedicines. 2023;11(5):1461.
122. Akai T, Hatta T, Sakata-Haga H, Yamamoto S, Otani H, Yamamoto S, et al. Cerebrospinal fluid may flow out from the brain through the frontal skull base and choroid plexus: a gold colloid and cadaverine injection study in mouse fetus. Child's Nervous Syst. 2021;37(10):3013–20.
123. Xie L, Kang H, Xu Q, Chen MJ, Liao Y, Thiyagarajan M, et al. Sleep drives metabolite clearance from the adult brain. Science. 2013;342(6156):373–7.
124. Bojarskaite L, Vallet A, Bjørnstad DM, Gullestad Binder KM, Cunen C, Heuser K, et al. Sleep cycle-dependent vascular dynamics in male mice and the predicted effects on perivascular cerebrospinal fluid flow and solute transport. Nat Commun. 2023;14(1):953.
125. Lee H, Xie L, Yu M, Kang H, Feng T, Deane R, et al. The effect of body posture on brain glymphatic transport. J Neurosci. 2015;35(31):11034–44.
126. Klarica M, Radoš M, Erceg G, Petošić A, Jurjević I, Orešković D. The influence of body position on cerebrospinal fluid pressure gradient and movement in cats with normal and impaired craniospinal communication. PLoS ONE. 2014;9(4): e95229.
127. Magnaes B. Body position and cerebrospinal fluid pressure. J Neurosurg. 1976;44(6):698–705.
128. Alperin N, Lee SH, Sivaramakrishnan A, Hushek SG. Quantifying the effect of posture on intracranial physiology in humans by MRI flow studies. J Magn Reson Imaging. 2005;22(5):591–6.
129. Alperin N, Burman R, Lee SH. Role of the spinal canal compliance in regulating posture-related cerebrospinal fluid hydrodynamics in humans. J Magn Reson Imaging. 2021;54(1):206–14.
130. Muccio M, Chu D, Minkoff L, Kulkarni N, Damadian B, Damadian RV, et al. Upright versus supine MRI: effects of body position on craniocervical CSF flow. Fluids Barriers CNS. 2021;18(1):61.
131. Young BA, Cramberg MJ. Treadmill locomotion in the American alligator (Alligator mississippiensis) produces dynamic changes in intracranial cerebrospinal fluid pressure. Sci Rep. 2022;12(1):11826.
132. Young BA, Greer S, Cramberg M. Slithering CSF: cerebrospinal fluid dynamics in the stationary and moving Viper Boa, Candoia aspera. Biology (Basel). 2021;10(7):672.
133. Smets NG, Strijkers GJ, Vinje V, Bakker ENTP. Cerebrospinal fluid turnover as a driver of brain clearance. NMR Biomed. 2023. https://doi.org/10.1002/nbm.5029.
134. Bakker ENTP, Naessens DMP, VanBavel E. Paravascular spaces: entry to or exit from the brain? Exp Physiol. 2019;104(7):1013–7.
135. Regodón S, Vivo JM, Franco A, Guillén MT, Robina A. Craniofacial angle in dolicho-, meso- and brachycephalic dogs: radiological determination and application. Ann Anat Anatomischer Anzeiger. 1993;175(4):361–3.
136. Brehm VH, Loeffler K, Komeyli H. Schädelformen beim Hund. Anat Histol Embryol. 1985;14(4):324–31.
137. Ekenstedt KJ, Crosse KR, Risselada M. Canine brachycephaly: anatomy, pathology. Genet Welfare J Comp Pathol. 2020;176:109–15.
138. Hecht EE, Smaers JB, Dunn WD, Kent M, Preuss TM, Gutman DA. Significant neuroanatomical variation among domestic dog breeds. J Neurosci. 2019;39(39):7748–58.
139. Colosimo C, Tartaro A, Cama A, Tortori-Donati P. The craniosynostoses. In: Tortori-Donati P, Rossi A, editors. Pediatric neuroradiology. Berlin, Heidelberg: Springer Berlin Heidelberg; 2005. p. 1289–315. https://doi.org/10.1007/3-540-26398-5_30.
140. Hussein AK, Sullivan M, Penderis J. Effect of brachycephalic, mesaticephalic, and dolichocephalic head conformations on olfactory bulb angle and orientation in dogs as determined by use of in vivo magnetic resonance imaging. Am J Vet Res. 2012;73(7):946–51.
141. Schmidt MJ, Volk H, Klingler M, Failing K, Kramer M, Ondreka N. Comparison of closure times for cranial base synchondroses in mesaticephalic, brachycephalic, and cavalier King Charles Spaniel Dogs. Vet Radiol Ultrasound. 2013;54(5):497–503.
142. Geiger M, Haussman S. Cranial suture closure in domestic dog breeds and its relationships to skull morphology. Anat Rec. 2016;299(4):412–20.
143. Sokołowski W, Czubaj N, Skibniewski M, Barszcz K, Kupczyńska M, Kinda W, et al. Rostral cranial fossa as a site for cerebrospinal fluid drainage—volumetric studies in dog breeds of different size and morphotype. BMC Vet Res. 2018;14(1):162.
144. Schmidt M, Ondreka N, Sauerbrey M, Volk H, Rummel C, Kramer M. Volume reduction of the jugular foramina in Cavalier King Charles Spaniels with syringomyelia. BMC Vet Res. 2012;8(1):158.
145. Flint G, Rusbridge C, editors. Syringomyelia. Berlin, Heidelberg: Springer Berlin Heidelberg; 2014.
146. Cappello R, Rusbridge C. Report from the Chiari-like malformation and syringomyelia working group round table. Vet Surg. 2007;36(5):509–12.
147. Knowler SP, Galea GL, Rusbridge C. Morphogenesis of canine Chiari malformation and secondary syringomyelia: disorders of cerebrospinal fluid circulation. Front Vet Sci. 2018;27:5.
148. Hechler AC, Moore SA. Understanding and treating Chiari-like malformation and syringomyelia in dogs. Top Companion Anim Med. 2018;33(1):1–11.
149. Rusbridge C. New considerations about Chiari-like malformation, syringomyelia and their management. In Pract. 2020;42(5):252–67.
150. Driver CJ, Rusbridge C, Cross HR, McGonnell I, Volk HA. Relationship of brain parenchyma within the caudal cranial fossa and ventricle size to syringomyelia in cavalier King Charles spaniels. J Small Anim Pract. 2010;51(7):382–6.
151. Couturier J, Rault D, Cauzinille L. Chiari-like malformation and syringomyelia in normal cavalier King Charles spaniels: a multiple diagnostic imaging approach. J Small Anim Pract. 2008;49(9):438–43.
152. Fenn J, Schmidt MJ, Simpson H, Driver CJ, Volk HA. Venous sinus volume in the caudal cranial fossa in Cavalier King Charles spaniels with syringomyelia. Vet J. 2013;197(3):896–7.
153. Cerda-Gonzalez S, Olby NJ, Griffith EH. Medullary Position At The Craniocervical Junction In Mature Cavalier King Charles Spaniels: relationship with neurologic signs and syringomyelia. J Vet Intern Med. 2015;29(3):882–6.
154. Cerda-Gonzalez S, Olby NJ, Griffith EH. Dorsal compressive atlantoaxial bands and the craniocervical junction syndrome: association with clinical signs and syringomyelia in mature cavalier King Charles Spaniels. J Vet Intern Med. 2015;29(3):887–92.
155. Cerda-Gonzalez S, Bibi KF, Gifford AT, Mudrak EL, Scrivani PV. Magnetic resonance imaging-based measures of atlas position: Relationship to canine atlantooccipital overlapping, syringomyelia and clinical signs. Vet J. 2016;209:133–8.
156. Bilston LE, Stoodley MA, Fletcher DF. The influence of the relative timing of arterial and subarachnoid space pulse waves on spinal perivascular cerebrospinal fluid flow as a possible factor in syrinx development. J Neurosurg. 2010;112(4):808–13.
157. Lloyd RA, Stoodley MA, Fletcher DF, Bilston LE. The effects of variation in the arterial pulse waveform on perivascular flow. J Biomech. 2019;90:65–70.
158. Martinac AD, Fletcher DF, Bilston LE. Phase offset between arterial pulsations and subarachnoid space pressure fluctuations are unlikely to drive periarterial cerebrospinal fluid flow. Biomech Model Mechanobiol. 2021;20(5):1751–66.

159. Elliott NSJ, Bertram CD, Martin BA, Brodbelt AR. Syringomyelia: a review of the biomechanics. J Fluids Struct. 2013;40:1–24.
160. Williams B. On the pathogenesis of syringomyelia: a review. J R Soc Med. 1980;73(11):798–806.
161. Bertram CD, Heil M. A poroelastic fluid/structure-interaction model of cerebrospinal fluid dynamics in the cord with syringomyelia and adjacent subarachnoid-space stenosis. J Biomech Eng. 2017. https://doi.org/10.1115/1.4034657.
162. Gonzalez SR, Light JG, Golinko MS. Assessment of epidemiological trends in craniosynostosis: limitations of the current classification system. Plast Reconstr Surg Glob Open. 2020;8(3): e2597.
163. Sadler B, Kuensting T, Strahle J, Park TS, Smyth M, Limbrick DD, et al. Prevalence and impact of underlying diagnosis and comorbidities on Chiari 1 malformation. Pediatr Neurol. 2020;106:32–7.
164. Ciaramitaro P, Garbossa D, Paola P, Piatelli G, Massimi L, Valentini L, et al. Syringomyelia and Chiari syndrome registry: advances in epidemiology, clinical phenotypes and natural history based on a North Western Italy cohort. Ann Ist Super Sanita. 2020;56(1):48–58.
165. Klimov VS, Gulay YUS, Evsyukov AV, Moysak GI. Syringosubarachnoid shunting in treatment of syringomyelia: a literature review and a clinical case report. Voprosy Neirokhirurgii Imeni NN Burdenko. 2017;81(3):58.

Publisher's Note